Improving the representation of cropland sites in the Community Land Model (CLM) version 5.0

Theresa Boas[1,2], Heye Bogena[1,2], Thomas Grünwald[3], Bernard Heinesch[4], Dongryeol Ryu[5], Marius Schmidt[1], Harry Vereecken[1,2], Andrew Western[5], Harrie-Jan Hendricks Franssen[1,2]

[1]Research Centre Jülich, Institute of Bio- and Geosciences: Agrosphere (IBG-3), 52425 Jülich, Germany
[2]Centre for High-Performance Scientific Computing in Terrestrial Systems: HPSC TerrSys, Geoverbund ABC/J, 52425 Jülich, Germany.
[3]Technische Universität Dresden (TU Dresden): Institute of Hydrology and Meteorology, 01062 Dresden, Germany
[4]University of Liège: Gembloux Agro-Bio Tech (GxABT), 5030 Gembloux, Belgium
[5]University of Melbourne: Department of Infrastructure Engineering, Parkville VIC 3010, Australia

Correspondence to: Theresa Boas (t.boas@fz-juelich.de)

Abstract. The incorporation of a comprehensive crop module in land surface models offers the possibility to study the effect of agricultural land use and land management changes on the terrestrial water, energy and biogeochemical cycles. It may help to improve the simulation of biogeophysical and biogeochemical processes on regional and global scales in the framework of climate and land use change. In this study, the performance of the crop module of the Community Land Model version 5 (CLM5) was evaluated at point scale with site specific field data focussing on the simulation of seasonal and inter-annual variations in crop growth, planting and harvesting cycles, and crop yields as well as water, energy and carbon fluxes. In order to better represent agricultural sites, the model was modified by (1) implementing the winter wheat subroutines after Lu et al. (2017) in CLM5; (2) implementing plant specific parameters for sugar beet, potatoes and winter wheat, thereby adding these crop functional types (CFT) to the list of actively managed crops in CLM5; (3) introducing a cover cropping subroutine that allows multiple crop types on the same column within one year. The latter modification allows the simulation of cropping during winter months before usual cash crop planting begins in spring, which is a common agricultural management technique in humid and sub-humid regions. We compared simulation results with field data and found that both the parameterization of the CFTs, as well as the winter wheat subroutines, led to a significant simulation improvement in terms of energy fluxes, leaf area index (LAI), net ecosystem exchange (RMSE reduction for latent and sensible heat by up to 57 % and 59 % respectively) and crop yield (up to 87 % improvement in winter wheat yield prediction) compared with default model results. The cover cropping subroutine yielded a substantial improvement in representation of field conditions after harvest of the main cash crop (winter season) in terms of LAI curve and latent heat flux (reduction of winter time RMSE for latent heat flux by 42 %). We anticipate that our model modifications offer opportunities to improve yield predictions, to study the effects of large-scale cover cropping on energy fluxes, soil carbon and nitrogen pools, and soil water storage in future studies with CLM5.

1 Introduction

Crop yield is highly influenced by environmental conditions – weather, nutrient availability, atmospheric CO_2 – and agricultural practices such as irrigation and fertilizer application. Global climate change is widely believed to have an important impact on future agriculture and consequently food security under changing climate is an important research topic (Lobell et al., 2011; Aaheim et al., 2012; Ma et al., 2012; Gosling, 2013; Rosenzweig et al., 2014). Numerous current crop yield predictions for the 21st century show declining global yield trends and

40   increasing irrigation requirements (Urban et al., 2012; Challinor et al., 2014; Deryng et al., 2014; Rosenzweig et al., 2014; Tai et al., 2014; Levis et al., 2018). General agricultural practices have adapted to changes in climate and inter-annual climate variability by adjusting irrigation amounts and fertilizer application as well as cultivating more resistant varieties of certain crops (Kucharik et al., 2006; Kucharik, 2008). Also, the biogeochemical effects and benefits of cover crops as well as their potential to mitigate climate change are the focus of many studies

45   (Sainju et al., 2003; Lobell et al., 2006; Plaza-Bonilla et al., 2015; Basche et al., 2016; Carrer et al., 2018; Lombardozzi et al., 2018; Hunter et al., 2019). The planting of cover crops is a common agricultural management practice in humid and sub-humid regions to reduce soil erosion, consolidation, and nitrogen leaching and to increase agricultural productivity by nitrogen fixation (Sainju et al., 2003; Lobell et al., 2006; Basche et al., 2014; Plaza-Bonilla et al., 2015; Tiemann et al., 2015; Kaye and Quemada, 2017).

50   With a trend of declining yield and increasing uncertainty in yields in many parts of the world, understanding the impact of climate change on crop production and improving the prediction of it is a research topic of great importance to society. Hence, the evaluation and advancement of integrated modelling approaches with adequate incorporation of crop phenology, the capacity to simulate realistic land management and crop yield in response to climate conditions on regional and global scale are the focus of many studies (Stehfest et al., 2007; Olesen et al.,

55   2011; Van den Hoof et al., 2011; Rosenzweig et al., 2014). The incorporation of a comprehensive crop module in land surface models offers the possibility to study changes in water and energy cycles and crop production in response to climate, environmental, land use, and land management changes and may help to improve the simulation of biogeophysical and biogeochemical processes on regional and global scales (Kucharik and Brye, 2003; Lobell et al., 2011; Lawrence et al., 2018).

60   The recent versions of CLM (i.e. 4.0, 4.5 and 5.0) adopted the prognostic crop module from the Agro-Ecosystem Integrated Biosphere Simulator (Agro-IBIS) (Kucharik and Brye, 2003), which has the ability to simulate the soil-vegetation-atmosphere system including crop yields, and has been evaluated in multiple studies (Twine and Kucharik, 2009; Webler et al., 2012; Xu et al., 2016). Even the simplified version of the Agro-IBIS crop scheme that was implemented in CLM4 led to improved simulation of climate-crop interactions and more comprehensive

65   ecosystem balances than previous CLM versions (Levis et al., 2012). Evaluation studies of CLM4 by Levis et al. (2012) and Chen et al. (2015) revealed significant sensitivities of energy and carbon fluxes to biases in crop phenology, especially for the seasonality of the net ecosystem carbon exchange for managed crop sites where the flux is governed by planting and harvest times. First evaluation studies of the CLM-Crop representation of plant hydraulics and its ability to represent crop growth cycles and ecosystem balance of crop sites are available by

70   Bilionis et al. (2015) for CLM4.5.

In the latest version, CLM (CLM5) has been extended with an interactive crop module that includes fertilizer and irrigation scheme, eight actively managed crop types (temperate soybean, tropical soybean, temperate corn, tropical corn, spring wheat, cotton, rice, and sugarcane), irrigated and unirrigated unmanaged crops. However, so far, only very few studies have evaluated CLM5 with respect to crop simulation performance (e.g. crop yield,

75   growth cycle representation and carbon budgets for agricultural ecosystems) either at single points or at regional and global scales (e.g. Chen et al., 2018; Sheng et al., 2018).

Chen et al. (2018) emphasize the importance of model performance evaluations at point scale over long timescales given that plant properties, soil properties and climate vary significantly between sites and the reliable simulation of long-term energy and carbon fluxes and variations in plant phenology remain an important challenge. An

80   assessment of the performance of CLM5 in simulating crop yields at the regional level was conducted by Sheng

et al (2018), who used CLM5 to simulate crop yield in northeast China. For maize, they found a general overestimation of LAI and an underestimation of stem and leaf carbon during the growing season, compared to observation data and statistical reports, as well as significant discrepancies in simulated and recorded harvesting and planting dates which resulted in a general overestimation of crop yield (Sheng et al., 2018).

85   The overall aim of this study is to evaluate and enhance the performance of the crop module of CLM5 focussing on the representation of seasonal and inter-annual variations in crop growth, planting and harvesting cycles, and crop yields as well as energy and carbon fluxes. Simulations were carried out for four cropland reference sites of the ICOS (Integrated Carbon Observation System) and TERENO (Terrestrial Environmental Observatory) networks in central Europe. In order to improve the representation of crop growth as well as energy fluxes on
90   agricultural fields at the point scale, several modifications were made within the code and the parameter configuration of the crop module. Firstly, we transferred and adapted the modified vernalization and cold tolerance routine by Lu et al. (2017) to the CLM5 code and tested it for several single point study sites. Secondly, modified parameter sets for winter wheat, sugar beet and potatoes were gathered from the literature and adopted from observation data and were tested at point scale. Finally, we extended CLM5 by adding a new cover cropping
95   subroutine that models the growth of winter cover crops and the rotation from a summer to a winter crop within the same year.

2   Materials and Methods

2.1   Community Land Model

In general, land surface models such as CLM5 are broadly applied in scientific studies to simulate water, energy
100   and nutrient fluxes in the terrestrial ecosystem (Niu et al., 2011; Han et al., 2014; Lawrence et al., 2018; Naz et al., 2019). CLM5 represents the latest version of the land component in the Community Earth System Model (CESM) (Lawrence et al., 2018). Within the model, simulated land surface fluxes such as latent and sensible heat are driven by atmospheric/meteorological input variables in combination with soil and vegetation states (e.g. soil moisture and LAI) and parameters (e.g. hydraulic conductivity, land cover) (Oleson et al., 2010; Lawrence et al.,
105   2011; Lawrence et al., 2018). The new biogeochemistry and crop module of CLM5 (BGC-Crop) adopted the prognostic crop module from the Agro-Ecosystem Integrated Biosphere Simulator (Agro-IBIS) (Kucharik and Brye, 2003). This incorporation of agriculturally managed land cover may help to improve the general representation of biogeochemical processes on the global scale to better address challenges from land use changes and agriculture practices (e.g. Lobell, Bala, and Duffy, 2006). The CLM5 crop module includes new crop
110   functional types, updated fertilization rates and irrigation triggers, a transient crop management option as well as some adjustments to phenological parameters. Also extensive modifications have been made to the grain C and N pool, e.g. C for annual crop seeding comes from the grain C pool and initial seed C for planting is increased from 1 to 3 gCm^{-2} (Lawrence et al., 2018).

Vegetated land units are separated into natural vegetation and crop land units, with only one CFT on each soil
115   column, including CFT specific land management techniques such as irrigation and fertilization (Lawrence et al., 2018). A total of 78 plant and crop functional types are included in CLM5 including an irrigated and unirrigated unmanaged C3 crop, eight actively managed crop types - spring wheat, temperate and tropical corn, temperate and tropical soybean, cotton, rice and sugarcane and 23 crop types without specific crop parameters associated that are merged to the most closely related and parameterised CFTs (Lawrence et al., 2018). For the simulation of those

120   inactive crop types, the specific crop parameters of the spatially closest and most similar out of the eight active crop types are used. Irrigation is simulated dynamically for defined irrigated CFTs in response to soil moisture conditions and is partly based on the implementation of Ozdogan et al. (2010) (Leng et al., 2013; Lawrence et al., 2018).

Besides water availability from irrigation and precipitation, crop yield and food productivity greatly depends on

125   fertilization. In CLM5-BGC-Crop, fertilization is represented by adding nitrogen directly to the soil mineral pool (Lawrence et al., 2018). Fertilization dynamics and annual fertilizer amounts depend on the crop functional types and vary spatially and yearly based on the Land Use Model Intercomparison Project (Lawrence et al., 2019) land use and land cover change time series. In CLM5, land fractions of natural vegetation are not influenced by fertilizer application. In cropping units, mineral fertilizer application starts during the leaf emergence phase of crop growth

130   and continues for 20 days. Manure nitrogen is applied at slower rates (0.002 kg N m^{-2} per year by default) to prevent rapid denitrification rates that were observed in earlier CLM versions so that more uptake by the plant is achieved.

CLM5-BGC-Crop is fully prognostic with regards to carbon and nitrogen in the soil, vegetation and litter at each time step. Allocation of assimilated carbon to the different segments of the plant (leaf, stem, root and reproductive

135   pool) is linked to the phenology phases and ends with the harvesting of the crop. The total amount of assimilated carbon is regulated by availability of soil nitrogen. The allocation of nitrogen is based on the specific C/N ratios in plant tissue that vary throughout the growing season and is therefore also related to crop phenology phases (Lawrence et al., 2018).

The crop phenology as well as the carbon and nitrogen cycling processes follow three phenology phases: phase

140   (1) from planting to leaf emergence, phase (2) from leaf emergence to beginning of grain fill and phase (3) from beginning of grain fill to maturity and harvest. These phenology phases are governed by temperature thresholds and the percentage of Growing Degree Days (GDD) required for maturity of the crop with harvest occurring when maturity is reached (Lawrence et al., 2018).

The first phenology stage, planting, starts when crop specific 10-day mean temperature thresholds (of both the

145   daily 2-m air temperature T_{10d} and the daily minimum 2-m air temperature $T_{min,10d}$) are met. The transition from planting to leaf emergence (phase 2) begins when the growing degree-days of soil temperature at 0.05 m depth (GDD_{Tsoi}) reaches 1 - 5 % of the GDD required for maturity (GDD_{mat}), depending on a crop specific base temperature for the GDD_{Tsoi}. Grain fill (phase 3) starts with either the simulated 2-m air temperature (GDD_{T2m}) reaching a heat unit threshold (h) of 40 – 65 % of GDD_{mat} or when the maximum leaf area index (L_{max}) is reached.

150   The crop is harvested in one time step when 100 % GDD_{mat} is reached or when the crop specific maximum number of days past planting is exceeded. The LAI is dependent on the specified specific leaf area (SLA) and the calculated leaf C. The SLA as well as the maximum LAI are specified for each crop in the parameter file (Table A2).

Allocation of assimilated carbon as well as the allocation to leaf, stem, root and reproductive pools is linked to the crop phenology phases and ends with harvest of the crop. The total amount of assimilated carbon is regulated by

155   availability of soil nitrogen, among other resources. The allocation of nitrogen is based on the specific C/N ratios in plant tissue (varying for roots, stem, leaves, reproductive pools) that vary throughout the growing season and are also related to crop phenology phases (Lawrence et al., 2018). Carbon allocation begins during leaf emergence and is specified using allocation coefficients which represent the fraction of available C that is available to be allocated to each C pool.

160   Nitrogen allocation of crops depends on the soil mineral nitrogen concentration and the crop specific C/N ratios
for each plant segment – leaves, stems, roots and reproductive organs. The nitrogen allocation scheme uses two
different C/N ratios for each crop based on the phenology stages to account for the generally lower C/N ratios
early in the growth cycle, higher ratios in later growth stages and the N retranslocation during grain fill.

For a detailed technical description of the model and all its features, the reader is referred to the technical
165   documentation of CLM5 (Lawrence et al., 2018).

2.2   Model modifications

In the course of this study, three main limitation of CLM5 for the intended simulation of agricultural sites in
Western Europe at point scale were identified: (1) the default CLM5-BGC-Crop code and parameterization yielded
a very poor representation of crop growth of winter wheat and other winter crops, (2) the default plant parameter
170   data set lacks specific parameterization for several important cash crops (here especially sugar beet and potatoes),
and (3) CLM5-BGC-Crop does not allow a second crop growth onset or a second CFT to be grown on the same
field within one year. These limitations were met by modifications to the code structure and parameterization of
the CLM5-BGC-Crop module described below.

2.2.1   Winter cereal representation

175   Vernalization (exposure to a period of non-lethal low temperatures required to enter the flowering stage for winter
crops) is a very significant process that distinguishes winter from summer cereal varieties. It influences the cold
tolerance of the crop and allows successful cultivation of winter crops during the colder months (Barlow et al.,
2015; Chouard, 1960). In general, the vernalization process ensures that the reproductive development of plants
growing over winter (winter crops and also natural vegetation) does not start in late summer or fall but rather in
180   late winter or spring.

Lu et al. (2017) introduced vernalization cold tolerance subroutines in CLM4.5 to better simulate winter cereal
LAI and grain yield. For this, they adapted the winter wheat vernalization model from Streck et al. (2003). Streck
et al. (2003) evaluated their vernalization algorithm for a wide range of winter wheat cultivars for the purpose of
being used in crop model approaches. The vernalization process starts after leaf emergence and ends before
185   flowering (Streck et al., 2003). The daily vernalization dependence is calculated based on the crown temperature
(T_{crown}) and the optimum vernalization temperature (T_{opt}) limited to times when the crown temperature lies within
the minimum to maximum vernalization temperature (T_{min} and T_{max}) range:

$$\alpha = \frac{ln2}{ln[(T_{max}-T_{min})/(T_{opt}-T_{min})]} \tag{1}$$

$$vd = \sum fvn(T_{crown}) = \frac{[2(T_{crown}-T_{min})^{\alpha}(T_{opt}-T_{min})^{\alpha}-(T_{crown}-T_{min})^{2\alpha}]}{(T_{opt}-T_{min})^{2\alpha}} \tag{2}$$

190    $$vf = \frac{vd^5}{22.5^5+vd^5} \tag{3}$$

where vd [-] is the sum of the sequential vernalization dependence, fvn [-] is the daily vernalization rate, vf [-] is
the vernalization factor, T_{crown} [K] is the crown temperature, T_{opt} [K], T_{max} [K] and T_{min} [K] are the optimum,
maximum and minimum vernalization temperatures respectively.

The crown temperature (T_{crown}) is assumed to be slightly higher than the 2-m air temperature (T_{2m}) in winter when
195   covered by snow. It is calculated separately for temperatures below and above the freezing temperature (T_{frz}):

$$T_{crown} = 2 + (T_{2m} - T_{frz}) * (0.4 + 0.0018 * (min(D_{snow} * 100,15) - 15)^2$$

for $T_{2m} < T_{frz}$ (4)

$$T_{crown} = T_{2m} - T_{frz}$$

for $T_{2m} > T_{frz}$ (5)

where T_{crown} [K] is the calculated crown temperature, T_{2m} [K] is the 2-m air temperature, T_{frz} [K] is the freezing point and D_{snow} [m] is the snow height.

The vernalization factor is then used in the cold tolerance subroutine to assess the cumulative cold hardening of the plant and its dehardening process when exposed to higher temperatures (see below) and in the adjustment of the GDDs since planting. The GDDs since planting as well as the allocation of C to the grain pool are multiplied by the vernalization factor at each time step. This leads to a reduced growth rate in the beginning of the phenology cycle when the plant is not fully vernalized ($vf < 1$).

Furthermore, Lu et al. (2017) implemented a cold tolerance subroutine using the approaches after Bergjord et al. (2008) and Vico et al. (2014). The damage from low temperatures is quantified by three main variables: the temperature at which 50 % of the plant is damaged (LT$_{50}$), the survival probability (f_{surv}) and winter killing degree days (WDD) (Bergjord et al., 2008; Lu et al., 2017; Vico et al., 2014). A detailed description of these approaches can be found in Bergjord et al. (2008) and Vico et al. (2014).

The temperature at which 50 % of the plant is damaged (LT$_{50}$) is calculated interactively at each time step depending on the previous time step and on several accumulative parameters. These parameters are the exposure to near-lethal temperatures (rate$_s$), the cold hardening or low temperature acclimation (contribution of hardening – rate$_h$), the loss of hardening due to the exposure to a period of higher temperatures (dehardening – rate$_d$) and stress due to respiration under snow (rate$_r$) that are each functions of the crown temperature (Lu et al., 2017 and references therein).

The survival rate (f_{surv}) is calculated as a function of LT$_{50}$ and the crown temperature. The probability of survival increases once the crown temperature is higher than LT$_{50}$ or decreases when it is lower (Vico et al., 2014):

$$f_{surv}(T_{crown}, t) = 2^{-\frac{T_{crown}}{LT_{50}}^{\alpha surv}} \tag{6}$$

The winter killing degree day (WDD) is calculated as a function of crown temperature and survival probability. When the survival probability and crown temperature are low, the WDD will be high (Vico et al., 2014).

$$WDD = \int_{winter} max[(T_{base} - T_{crown}), 0] \; [1 - f_{surf}(T_{crown}, t)] dt$$

where $T_{base} = 0 \, °C$.   (7)

Lower LT$_{50}$ indicate a higher frost tolerance and would result in higher survival rates and thus smaller WDD and less cold damage to the plant.

Lu et al. (2017) implemented a relationship between frost damage described above and the subsequent growth or carbon allocation of the plant. Whenever the survival factor is less than 1, a small amount of leaf carbon (5 g C m^{-2} per model time step) as well as a small amount of leaf nitrogen (scaled by the prescribed C/N target ratios, Table 1 and Table A2) are transferred to the soil carbon and nitrogen litter pool thus simulating a reduction in growth and/or damage of small/young leaves and seedlings. Additionally, in order to simulate more drastic and instantaneous damage or death of the plant due to a longer duration of lethal temperatures (most likely to occur in spring when the plant has emerged and is close to or already fully vernalized), a second frost damage function is implemented. When WDD > 1° days the frost damage function is triggered, leading to severe crop damage by transferring leaf carbon (amount scaled by the survival probability (1 -f_{surv})) to the soil carbon litter pool.

2.2.2 Extended Parameterization

Table 1: CFT specific phenology and CN allocation parameters.

Parameter	CLM variable name	Units
Phenology		
Minimum planting date for the Northern Hemisphere	min_NH_planting_date	MMDD
Maximum planting date for the Northern Hemisphere	max_NH_planting_date	MMDD
Average 5 day daily temperature needed for planting	planting_temp	K
Average 5 day daily minimum temperature needed for planting	min_planting_temp	K
Minimum growing degree days	gddmin	°days
Maximum number of days to maturity	mxmat	Days
Growing Degree Days for maturity	hygdd	°days
Base Temperature for GDD	baset	°C
Maximum Temperature for GDD	mxtmp	°C
Percentage of GDD for maturity to enter phase 3	lfemerg	% GDDmat
Percentage of GDD for maturity to enter phase 4	grnfill	% GDDmat
Canopy top coefficient	ztopmax	M
Maximum Leaf Area Index	laimx	m^2/m^2
Specific Leaf Area	slatop	m^2/gC
CN ratios and allocation		
Leaf C:N	leafcn	gC/gN
Minimum leaf C:N	leafcn_min	gC/gN
Maximum leaf C:N	leafcn_max	gC/gN
Fine root C:N	frootcn	gC/gN
Grain C:N	graincn	gC/gN
Fraction of leaf N in Rubisco	flnr	fraction/gNm^{-2}

In order to yield a reasonable representation of agricultural areas on the regional scale in future studies, the default
240   parameter set was extended with specific crop parameters for sugar beet, potatoes, and winter wheat based on the
characteristics of our study sites to better fit the observed plant phenology and energy fluxes at the simulation sites.
In selecting parameters to be modified, the sensitivity analysis and parameter estimation studies by Post et al.
(2017) (for version 4.5), Cheng et al. (2020) and Fisher et al. (2019) (for version 5.0) were taken into account. Key
parameters as identified by previous studies (Sulis et al., 2015; Post et al., 2017; Lu et al., 2017; Fisher et al., 2019;
245   Cheng et al., 2020) are listed in Table 1. These parameters were adjusted with values from the literature or site-
specific observations to match observed values. General phenology parameters such as the maximum canopy
height, planting temperatures, maximum LAI, maximum and minimum planting dates and days for growing were
adjusted according to field documentation data and the respective site planting and harvest dates. Records on
planting and harvest dates as well as crops that were planted for all study sites are listed in Table A1. C/N ratios
250   in leaves and roots for wheat and sugar beet were adapted from Whitmore and Groot (1997), Gan et al. (2011),
Sánchez-Sastre et al. (2018) and Zheng et al. (2018). The specific leaf area (slatop) and the fraction of leaf N in
Rubisco (flnr) for sugar beet and winter wheat were taken from Sulis et al. (2015) and references therein and
adopted also for potatoes. A full list of default and modified parameters for the CFTs temperate corn, spring wheat,
sugar beet, potatoes and winter wheat can be found in Table A2.

2.2.3   Cover cropping scheme

255

The effect of cover crops on the physical and biogeochemical properties of the land surface alters latent heat flux, albedo and soil carbon and nitrogen storage and can potentially impact local and regional climate (Sainju et al., 2003; Lobell et al., 2006; Möller and Reents, 2009; Plaza-Bonilla et al., 2015; Basche et al., 2016; Carrer et al., 2018; Lombardozzi et al., 2018; Hunter et al., 2019).

260

In the default BGC phenology, the growth algorithm starts in the beginning of each year, when the crop is not alive on the specific patch. Furthermore, the CLM structure does not allow multiple CFTs to coexist on the same column so that multiple planting phases related to cover cropping over winter months or crop rotations with winter and summer crops, both being very common practices in Europe and worldwide, cannot be accounted for. This might also be an issue when representing ecosystems where agricultural management practices involve multiple sowing

265

and harvest cycles in accordance with the monsoon season (e.g. India). Therefore, a cover cropping subroutine was implemented in the BGC phenology module that affects the onset/offset (crop cycle/fallow) algorithm to allow a second onset period (crop cycle) on the same column.

A cover crop flag was introduced in the parameter file and in the source code. This flag can be set for any CFT in the parameter file and calls the cover-cropping subroutine when it is set to true (covercrop_flag $\neq 0$). This allows

270

a flexible handling of this option as well as an application on a larger scale. With this modification, the onset period can start again within one simulation year for another (or the same) CFT. For example, when the maturity of the crop is reached and it has been harvested, the model would by default switch to the next stage (phase 4) where the crop is not alive and the offset (fallow) period begins. The next onset period and GDD accumulation for planting would then start in the subsequent simulation year. In our modified CLM5 version, the cover-cropping

275

subroutine is called before entering into the offset period when the cover-crop flag for the current CFT is set to true. In the cover-cropping subroutine, the CFT is then changed according to a predefined rotation scheme and another onset period and GDD accumulation for planting is initialized.

First, the new subroutine was tested for a hypothetical rotation of two cash crops (spring wheat and sugar beet), allowing a green stubble to evolve over winter rather than simulating bare soil. Secondly, two realistic scenarios

280

were tested for DE-RuS. From 2016 to 2017, planting was altered at DE-RuS from barley (here represented by the CFT for spring wheat) in 2016 to sugar beet in 2017 with a greening mix cover crop coverage (winter months 2016/2017) in between. The catch crop was ploughed into the soil prior to the planting of sugar beet in 2017. In order to simulate this common cover cropping practice, we implemented a new CFT greening mix (or catch crop 1). For this CFT, the CN allocation algorithm was changed in such way that, when the plant reaches maturity, the

285

plant carbon and nitrogen are transferred to the soil litter pool and not allocated to the food product pool. For the years 2017 to 2019 at DE-RuS, the subroutines ability to simulate realistic crop rotation cycles was tested by changing the simulated CFT from sugar beet (2017) to winter wheat (2017-2018) and then to potatoes (2019). This possibility to change the CFT within the same year represents a significant improvement of CLM, since CLM5 only permits land use changes at the beginning of every year.

290

2.3   Study sites and validation data

Table 2: ICOS and TERENO cropland study site location coordinates and altitude (Alt.), soil types, Köppen-Geiger climate classification (Peel et al., 2007), mean annual temperature (T), mean annual precipitation amounts (P) and reference.

Site/ID	Project	Location	Alt. [msl]	Soil type	Climate	T [°C]*	P [mm/a]*	Ref.

Selhausen DE-RuS	TERENO ICOS	50.865°N 6.447°E	104.5	Luvisol	Cfb - temperate maritime	9.9	698	Ney et al. (2017)
Merzenhausen DE-RuM	TERENO	50.930°N 6.297°E	100	Cambisol	Cfb - temperate maritime	9.9	698	Bogena et al. (2018)
Klingenberg DE-Kli	ICOS	50.893°N 13.522°E	478	Gleysoil	Cfb – suboceanic, subcontinental	8.1	766	Grünwald (personal communication, 2020)
Lonzée BE-Lon	ICOS	50.553°N 4.746°E	167	Luvisol	Cfb - temperate maritime	10	800	Buysse et al.(2017)

* Reference periods: 1961-2010 for DE-RuS (adapted also for DE-RuM), 2005-2019 for DE-Kli and 2004-2017 for BE-Lon.

Site-specific measurement records of latent and sensible heat fluxes, net ecosystem exchange (NEE), LAI, soil
295   temperature and soil moisture were used as validation data. The sites (Selhausen, Merzenhausen, Klingenberg and
Lonzée) were selected mainly for their excellent meteorological records and validation data.

Selhausen (50.86589°N, 6.44712°E) is part of the TERENO Rur Hydrological Observatory (Bogena at al., 2018)
as well as the Integrated Carbon Observation System (ICOS, 2020). The test site covers an area of approximately
1 km x 1 km and is located in the lower Rhine valley (Bogena et al., 2018). Selhausen had a crop rotation of sugar
300   beet (*Beta vulgaris*), winter wheat (*Triticum aestivum*) and winter barley (*Hordeum vulgare*), fewer times also
rapeseed (*Brassica napus*) and potatoes (*Solanum tuberosum*) from 2015 to 2019. Cover crops such as oilseed
radish or catch crop mixes are planted occasionally between two main crop rotations. Continuous records of
meteorological variables, soil specific observations, greenhouse gas and energy fluxes are available for Selhausen
since 2011. Regular LAI measurements are available since 2016 (Ney and Graf, 2018).

305   Merzenhausen (50.93033°N, 6.29747°E) is located at approximately 14 km from Selhausen and is also part of the
TERENO Rur Hydrological Observatory. The crop rotation of the site includes sugar beet (*Beta vulgaris*), winter
wheat (*Triticum aestivum*), winter barley (*Hordeum vulgare*), rape seed (*Brassica napus*) and occasionally catch
crops mixes. For Merzenhausen, continuous records of meteorological variables, soil specific observations and
energy fluxes are available since 2011 and LAI measurements from 2016 – 2018.

310   Klingenberg (50.89306°N, 13.52238°E) is an ICOS cropland site located in the mountain foreland of the
Erzgebirge that is operated by the Technical University Dresden (TU Dresden) (ICOS, 2020; Prescher et al., 2010).
The site is characterized as managed cropland with a 5-year planting rotation of rapeseed (*Brassica napus*), winter
wheat (*Triticum aestivum*), maize (*Zea mays*), spring and winter barley (*Hordeum vulgare*) (Kutsch et al., 2010).
Since 2004, data on ecosystem fluxes (including net ecosystem and net biome productivity), meteorological
315   variables and soil observations are collected. Furthermore, biomass observations and agricultural management
information are available for this site.

The cropland site Lonzée (50.553°N 4.746°E) in Belgium is also part of ICOS (Buysse et al., 2017). It has been
planted in a four-year rotation cycle with sugar beet (*Beta vulgaris*), winter wheat (*Triticum aestivum*), potato
(*Solanum tuberosum*), winter wheat (*Triticum aestivum*) since 2000 with Mustard as a cover crop after winter
320   wheat harvest (Moureaux, 2006; Moureaux et al., 2008). For Lonzée, continuous records of meteorological
variables, EC flux data and LAI (GLAI and GAI) measurements are available from 2004 onwards. General
information on the ICOS study sites such as climatic conditions, soil types etc. is provided on the ICOS Carbon
Portal under the respective site codes (ICOS, 2020).

At all sites, the application of mineral fertilizer and herbicides/pesticides as well as occasional application of
325   organic fertilizer is regular management practice.
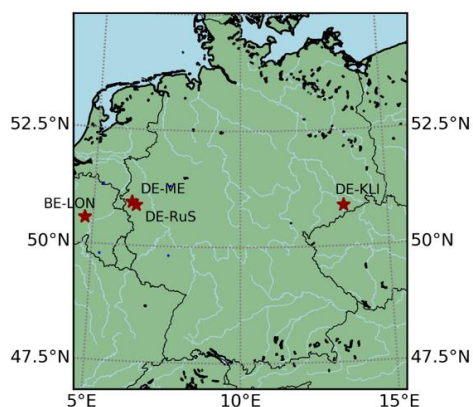
Figure 1: ICOS and TERENO cropland study sites Selhausen (DE-RuS), Merzenhausen (DE-RuM), Klingenberg (DE-Kli) and Lonzée (BE-Lon)

Station data required to force CLM, i.e. meteorological variables (see following section) were measured as block
330 averages over 10 minutes or at higher resolutions, gap-filled using linear statistical relations to nearby stations
where possible (Alexander Graf, 2017), or otherwise, by marginal distribution sampling within the software
package REddyProc (Wutzler et al., 2018). Fluxes required for model validation (i.e. net ecosystem CO_2 exchange
(NEE), latent heat flux (LE), sensible heat flux (H), soil heat flux (G) and gross primary production (GPP)) and
net radiation (Rn), were either measured (G and R_n) or computed from turbulent raw measurements (frequency $\geq$
335 10 s^{-1}) using the eddy-covariance method, for 30-minute block averages by the site PIs. Subsequently, gaps were
filled and GPP estimated from NEE using REddyProc (Wutzler et al., 2018). More details on quality control,
filling of longer gaps and by nearby stations, correction of soil heat flux and energy balance closure analysis are
given in Graf et al. (*in review*) and specifically for DE-RuS and DE-RuM including LAI measurements in
Reichenau et al. (2020). The long-term annual energy balance closures of the sites DE-RuS, DE-Kli and BE-Lon
340 were approximately 79%, 77% and 76%, respectively, according to analyses in Graf et al. (*in review*) and 76% at
DE-RuM according to an earlier study by Eder et al. (2015). All half-hourly meteorological and flux data were
aggregated to hourly averages to match the customized CLM time step. Forcing variables were always used in
gap-filled form, while validation variables were used in un-filled, quality-filtered form.

3   Experimental design and analyses

3.1   Model implementation

345

For the single point study sites, CLM was run in point mode with only one grid cell and forced with site specific
hourly meteorological data.

The annual fertilization amounts at the single point study sites were adjusted according to documented amounts of
applied fertilizer that ranged between 12 and 20 gNm⁻². In CLM5, the potential photosynthetic capacity as well as
350 the total amount of assimilated carbon during the phenology stages are regulated by the availability of soil nitrogen
(Lawrence et al., 2018). With modern fertilization practices in Europe, nitrogen is not assumed to represent a
limiting factor for the studied sites.

In order to balance ecosystem carbon and nitrogen pools, gross primary production and total water storage in the system, a spin-up is required (Lawrence et al., 2018). An accelerated decomposition spin-up of 600 years and an
355 additional spin-up of 400 years was conducted for each site with the BGC-Crop module active (Lawrence et al., 2018; Thornton and Rosenbloom, 2005). The resulting restart file at the end of the spin-up was then used as initial conditions for the following simulations.

Table 3: Overview of conducted simulation test runs and scenarios for the three main modifications (1) winter cereal representation, (2) parameterization and (3) cover cropping scheme listing the respective sites, simulation periods, simulated
360 CFTs, number of runs and different model versions and parameterizations that were run. CLM_D indicates the default model version, CLM_WW is the modified winter wheat model, and CLM_WW_CC is the modified winter wheat model extended with the cover cropping subroutine. The options *d* and *m* imply usage of the default or modified parameter set respectively.

Site	Simulation year(s)	Simulated CFT	Nr. of runs	Model version	Parameter set
1 Winter cereal representation					
DE-RuS	2017/2018	Winter wheat	2	CLM_D CLM_WW	*d* *m*
DE-RuM	2016/2017	Winter wheat	2	CLM_D CLM_WW	*d* *m*
DE-Kli	2005/2006 2010/2011 2015/2016	Winter wheat	2	CLM_D CLM_WW	*d* *m*
BE-Lon	2006/2007 2008/2009 2010/2011 2012/2013 2014/2015 2016/2017	Winter wheat	2	CLM_D CLM_WW	*d* *m*
2 Parameterization					
DE-RuS	2017	Sugar beet	2	CLM_WW	*d* *m*
DE-RuS	2019	Potato	2	CLM_WW	*d* *m*
DE-Kli	2018	Temperate corn	1	CLM_WW	*d*
BE-Lon	2008 2016	Sugar beet	2	CLM_WW	*d* *m*
BE-Lon	2010 2014 2018	Potato	2	CLM_WW	*d* *m*
3 Cover cropping scheme					
DE-RuS	2016 – 2017	Barley Cover crop 1 - greening mix Potato	2	CLM_D CLM_WW_CC	*d* *m*
DE-RuS	2017 – 2019	Sugar beet Winter wheat Potatoes	2	CLM_D CLM_WW_CC	*d* *m*

To test the first modification, the implementation of the winter cereal representation, single point simulations were
365 run with the default model version and with the modified model. The default model uses the standard and modified parameter set for winter wheat as input, while the modified model uses the modified parameter set for all winter wheat years. Simulations are performed for DE-RuS, DE-Kli, BE-Lon and DE-RuM (see Table 3). The modified CLM_WW is further used and extended in the subsequent steps.

For testing of the second modification, the parameterization of sugar beet and potatoes, simulations were run with
370 both the default and the modified parameter set for sugar beet and potatoes at the sites DE-RuS and BE-Lon. Furthermore, the default parameterization of the active CFT for corn was tested for the site DE-Kli (Table 3).

The third modification, the cover cropping scheme, was tested for the cropland site DE-RuS (Table 3). In this step, the CLM_WW model was further extended with the cover cropping subroutine (CLM_WW_CC) and the simulations were run with the previously modified and tested parameter set of crop specific parameters.

375   CLM_WW_CC simulation results were then compared to default model simulation results (CLM_D) using site specific validation data.

3.2   Evaluation of model performance

For statistical evaluation of the model results, the root mean square error (RMSE), the bias (BIAS) and the Pearson correlation (r) were chosen as performance metrics:

380      $RMSE = \sqrt{\frac{1}{n}\sum_{i=1}^{n}(X_i - X_{obs,i})^2},$ (8)

$BIAS = \sum_{i=1}^{n}(X_i - X_{obs,i})/\sum_{i=1}^{n}(X_{obs,i}),$ (9)

$r = (\frac{1}{n}\sum_{i=1}^{n}(X_{obs,i} * X_i) - \mu_{sim} * \mu_{obs})/(\sigma_{sim} * \sigma_{obs}),$ (10)

where i is time step and n the total number of time steps, X_i and $X_{obs,i}$ are the simulated and the observed values at every time step with μ_{sim} and μ_{obs} being the respective mean values. The standard deviation of simulation results

385   and measurement data are represented by σ_{sim} and σ_{obs} respectively.

The statistical evaluation was conducted for daily simulation output and daily observation data for the variables NEE, LE, H and Rn.

4   Results

4.1   Winter cereal representation

390   For all study sites and simulation years, CLM_WW simulations resulted in a much better representation of the growth cycle and corresponding seasonal LAI variation and magnitudes compared with CLM_D simulations (Figures 2-5). As described by Lu et al. (2017), the default vernalization routine reaches a factor of 1 (fully vernalized) shortly after planting when the first frost occurs. This induced an unrealistically early commencement of the grain fill stage within two months after planting (November or December). The peak in LAI in the default

395   version is also reached early in the year where photosynthesis is generally lower. The adapted CLM_WW vernalization routine produces lower initial vernalization factors which reduce the growing degree days. This leads to later onset of the leaf emergence and grain fill stage, in line with observations for all simulated study sites and years (Figures 2-5). While the planting date is the same for CLM_D and CLM_WW simulations, CLM_WW generally resulted in a better match of simulated and recorded harvest dates, compared with CLM_D simulations

400   (1.5 to 2 months later than CLM_D), but harvest is still simulated slightly too early for all sites (Table 4).
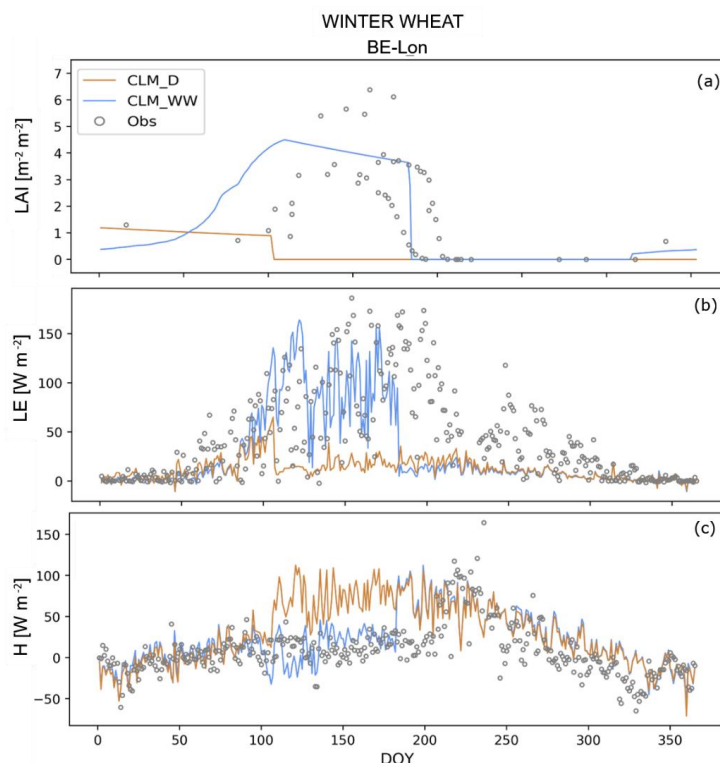
Figure 2: Daily simulation results of (a) LAI, (b) LE and (c) H averaged over all winter wheat years (see Table 5) at the BE-Lon site. Simulations were run with the default model version (CLM_D) indicated in orange and the modified model version (CLM_WW) indicated in blue. Site observation data on GLAI (all available observations plotted) and fluxes (averaged over

405 all respective years) are indicated in grey. Corresponding performance statistics for daily simulation results are listed in Table 5.

For the BE-Lon site, CLM_WW simulated average LAI peak magnitudes, as well as seasonal LAI variations, are close to the observations of the green leaf area index (GLAI), with the exception of 2015, where unusually high GLAI values where observed in May and June, ranging from 5.40 to 6.38 m^2/m^2. The LAI peak of CLM_WW

410 happens approximately one month too early compared to observations, and thus, the maturity of the crop is reached too early. This is also reflected in CLM_WW planting and harvest dates that are simulated approximately 1 month earlier than recorded dates. The CLM_WW simulated latent heat flux is underestimated after the crop cycle has ended in simulations compared to actual field conditions, where the crop is harvested later and thus more latent heat is generated on the field (Table 4, Figure 2). Although simulated maximum LAI generally correspond

415 reasonable with observed values, the resulting crop yield is underestimated compared to site harvest records (Table 4). While CLM_D simulations underestimated the grain yield by approximately 85 – 90 %, CLM_WW underestimated yield by only 18 - 36 %. The CLM_WW simulated yields show only minimal variations with values from 8.12 to 8.16 t/ha whereas measured yields range from 9.92 to 12.88 t/ha. Therefore, CLM_WW did not capture the inter-annual differences in yield very well (Table 4).

420 As observed for the BE-Lon site, CLM_WW overestimated early growing season LAI at the DE-RuS and DE-RuM sites with the simulated peak and subsequent slow decline in LAI happening earlier than observed values

(Figure 3 and 4). At the DE-RuS site, the generally good correspondence in growing cycle and LAI of the CLM_WW simulation is also reflected in the resulting crop yield of 9.15 t/ha that is very close to the observed value of 9.2 t/ha, while CLM_D strongly underestimated yield (1.17 t/ha).

425
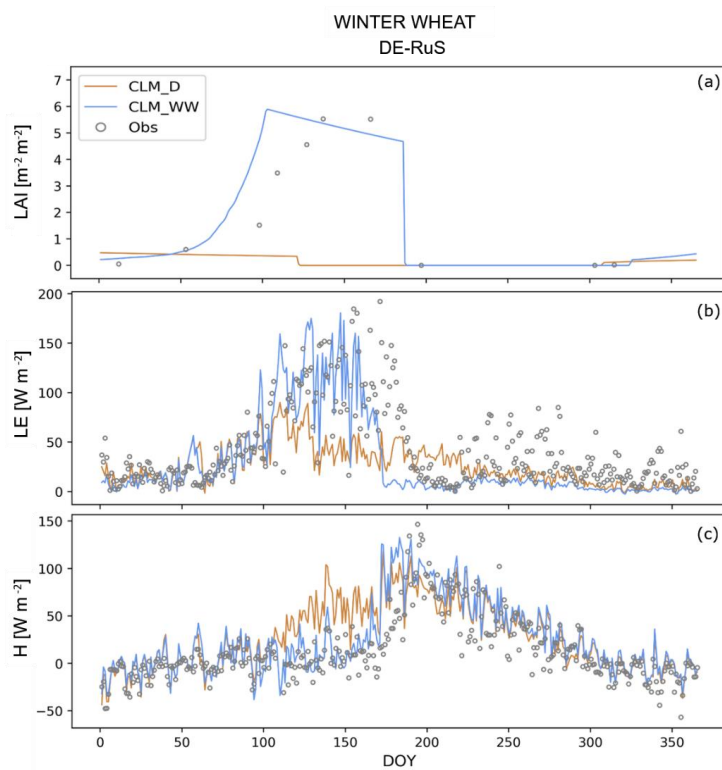
Figure 3: Daily simulation results of (a) LAI, (b) LE and (c) H for the winter wheat year 2018 at the DE-RuS site. Simulations were run with the default model version (CLM_D) indicated in orange and the modified model version (CLM_WW) indicated in blue. Site observation data on LAI (all available observations plotted) and fluxes (averaged over all respective years) are indicated in grey. Corresponding performance statistics for daily simulation results are listed in Table 5.

430
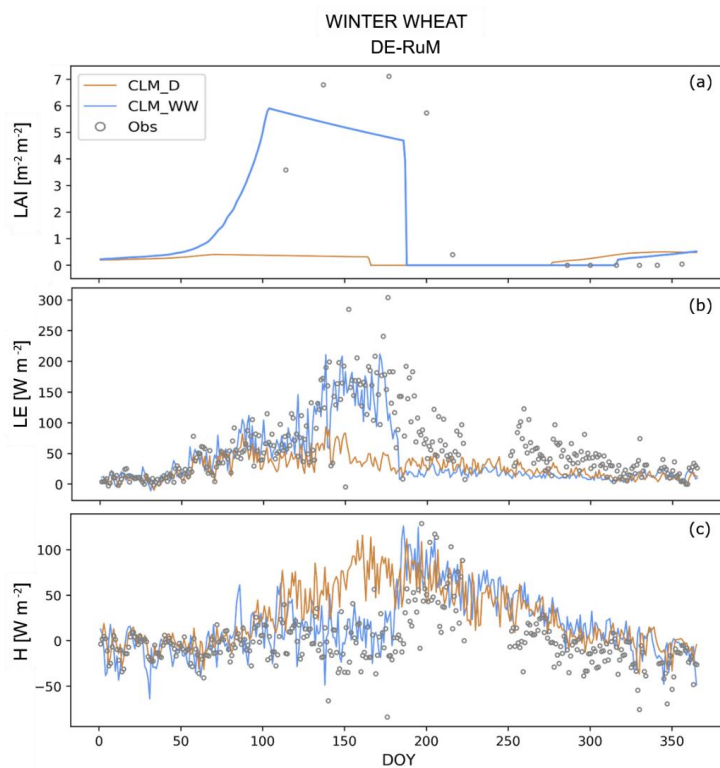
Figure 4: Daily simulation results of (a) LAI, (b) LE and (c) H for the winter wheat year 2017 at the DE-RuM site. Simulations were run with the default model version (CLM_D) indicated in orange and with the modified model version (CLM_WW) indicated in blue. Site observation data on LAI (all available observations plotted) and fluxes (averaged over all respective years) are indicated in grey. Corresponding performance statistics for daily simulation results are listed in Table 5.

For the DE-Kli site (Figure 5), site-specific observations of the LAI are not available. However, CLM_WW resulted in much more realistic magnitudes of LAI than CLM_D simulations. The generally lower LAI peak of CLM_WW compared to the other two sites is also reflected in lower crop yields for DE-Kli. Here, CLM_WW simulated crop yields match recorded yield data very well for the year 2011 and are overestimated for 2016 by approximately 16 %. CLM_D resulted in an underestimation of yield by more than 80 %.
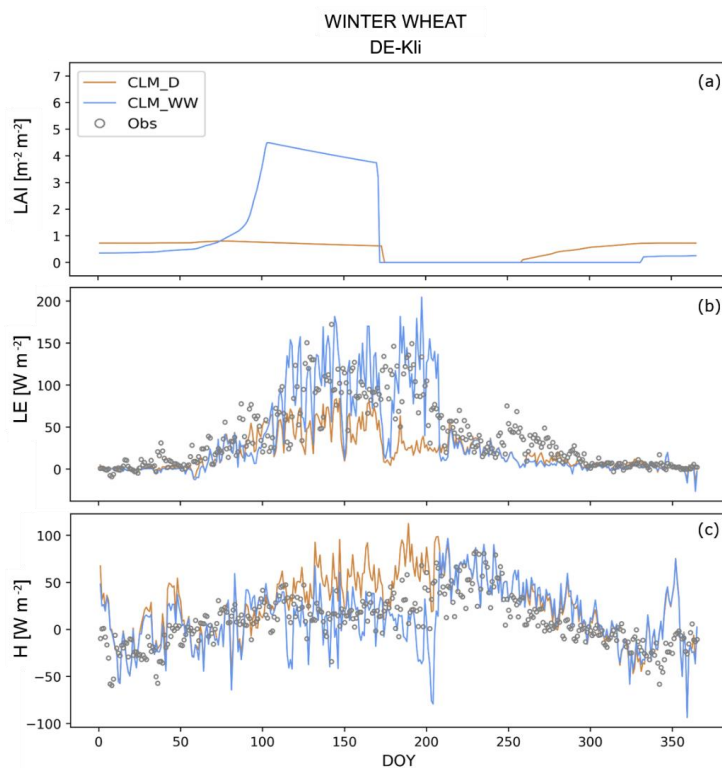
445

Figure 5: Daily simulation results of (a) LAI, (b) LE and (c) H averaged over all winter wheat years (see Table 5) at the DE-Kli site. Simulations were run with the default model version and the default parameter set (CLM_D) indicated in orange and the modified model version (CLM_WW) indicated in blue. Site observation data on LAI (all available observations plotted) and fluxes (averaged over all respective years) are indicated in grey. Corresponding performance statistics for daily simulation

450   results are listed in Table 5.

The generally better representation of the winter wheat growing cycle by CLM_WW is also reflected in simulated NEE (Figure 6) and surface energy fluxes (Figures 2-5). In terms of net radiation, both CLM_WW and CLM_D are very close to the observations (Table 5). However, CLM_WW was able to better capture seasonal variations in cumulated monthly sums of surface energy fluxes during the growing cycle of the crop. The correlation
455   coefficients for the energy fluxes (LE, H and Rn) calculated over the timeframe from recorded planting to harvest date (Table 4) improved for all sites (Table 5). Highest correlations were reached for the sites DE-Kli with r values of 0.62 and 0.71 and for BE-Lon with r values of 0.5 and 0.46 for sensible heat and latent heat flux respectively (Table 5). While the correlation of these variables is generally increased with the CLM_WW model, latent and sensible heat flux RMSE and biases are still relatively high, especially for the BE-Lon site, with corresponding
460   low correlations. The high latent heat flux measured at BE-Lon in the later months of the year (from day 220 onwards) reflects a second growth cycle of a cover crop. At both the BE-Lon site as well as at the DE-Kli site, catch crops are typically sown after harvest of winter wheat (mustard at BE-Lon, radish and brassica at DE-Kli) which strongly effects surface energy fluxes later in the year, whereas in CLM, the crop field is simulated as fallow (Figures 2 and 5).

465 Table 4: Simulated annual planting and harvest dates and grain yield [tDM/ha] by CLM_WW and CLM_D simulations compared to recorded harvest dates and grain yield (Obs) for all simulated winter wheat years at the sites BE-Lon, DE-RuS, DE-RuM and DE-Kli. For CLM simulation results, grain yield is calculated from grain carbon which is assumed to be 45 % of the total dry weight.

Year	Source	Planting date	Harvest date	Grain Yield [tDM/ha]
		BE-Lon		
	CLM_D	11.09.2010	10.05.2011	1.71
2010/2011	CLM_WW	11.09.2010	05.07.2011	8.14
	Obs	*14.10.2010*	*16.08.2011*	*10.64**
	CLM_D	12.09.2012	19.04.2013	1.68
2012/2013	CLM_WW	12.09.2012	25.06.2013	8.16
	Obs	*25.10.2012*	*12.08.2013*	*12.88*
	CLM_D	09.09.2014	20.04.2015	1.71
2014/2015	CLM_WW	09.09.2014	01.07.2015	8.15
	Obs	*15.10.2014*	*02.08.2015*	*11.13*
	CLM_D	11.09.2016	02.05.2017	1.68
2016/2017	CLM_WW	11.09.2016	24.07.2017	8.12
	Obs	*29.10.2016*	*30.07.2017*	*9.92*
		DE-RuS		
	CLM_D	29.09.2017	17.05.2018	1.17
2017/2018	CLM_WW	29.09.2017	27.06.2018	9.15
	Obs	*25.10.2017*	*16.07.2018*	*9.2*
		DE-RuM		
	CLM_D	27.09.2016	15.05.2017	1.45
2016/2017	CLM_WW	27.09.2016	30.06.2017	9.65
	Obs	*17.10.2016*	*22.07.2017*	*-*
		DE-Kli		
	CLM_D	15.09.2009	23.07.2011	1.19
2010/2011	CLM_WW	15.09.2009	11.08.2011	7.53
	Obs	*02.10.2010*	*22.08.2011*	*6.12*
	CLM_D	17.09.2015	24.07.2016	1.17
2015/2016	CLM_WW	17.09.2015	28.07.2016	7.44
	Obs	*18.09.2015*	*24.08.2016*	*7.48*

*: Grain yield estimated from 18.09 t/ha total biomass (stem and ear) yield according to stem and ear (grain) biomass yield
470 ratios measured for other winter wheat years at the same site.

CLM_WW was generally better able to match NEE observations compared to CLM_D due to the better representation of the seasonal LAI variations (Figure 6). Correlation improved (comparing CLM_WW to CLM_D) from 0.13 to 0.46 for BE-Lon, from 0.21 to 0.33 for DE-RuS and from 0.29 to 0.56 for DE-Kli. The resulting correlation for CLM_WW simulations is still relatively low due to an underestimation of the cumulative monthly

475 NEE during seasons with high NEE at both sites. For DE-Kli, CLM_WW was able to match NEE observed at peak LAI very well. However, late seasonal NEE (July), shortly before harvest, is overestimated by CLM_WW resulting in a low overall agreement with observation data.
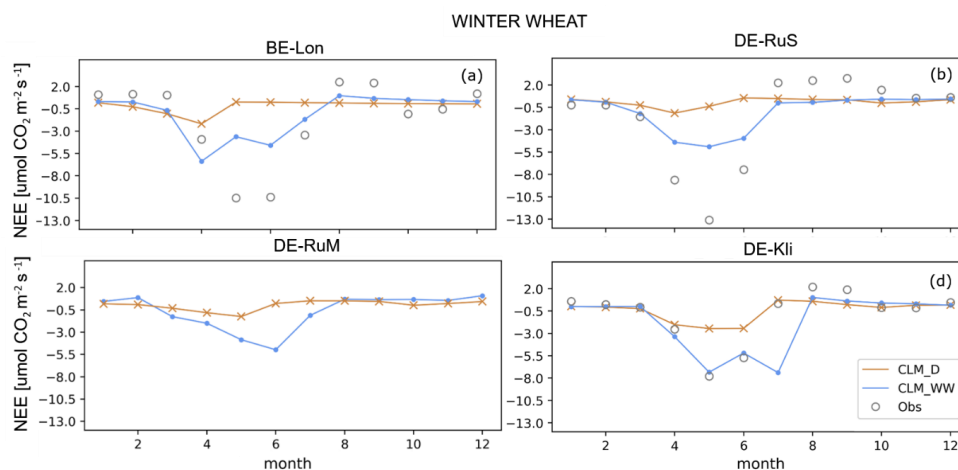
Figure 6: Comparison of (orange) CLM_D and (blue) CLM_WW simulated monthly NEE rates at the sites (a) BE-Lon, (b)
480   DE-RuS, (c) DE-RuM and (d) DE-Kli for all respective winter wheat years. Available site observations are plotted as grey
circles. For the sites BE-Lon and DE-Kli, simulation results as well as observation data is averaged over all simulated winter
wheat years.

Table 5: Bias, root mean square error (RMSE) and Pearson correlation coefficient (r) for the CLM_D and CLM_WW simulated
daily NEE [umol CO_2 W m^{-2} s^{-1}], LE [W m^{-2}], H [W m^{-2}] and Rn [W m^{-2}] at the sites BE-Lon, DE-RuS, DE-RuM and DE-Kli
485   respectively. Values were calculated for the time between recorded planting and harvest dates (averaged over all winter wheat
years at each site) using simulation output and observation data at daily time step.

CFT	WINTERWHEAT							
Site	BE-Lon		DE-RuS		DE-RuM		DE-Kli	
Year(s)	2006/2007 2008/2009 2010/2011 2012/2013 2014/2015 2016/2017		2017/2018		2016/2017		2010/2011 2015/2016	
Model	CLM_D	CLM_WW	CLM_D	CLM_WW	CLM_D	CLM_WW	CLM_D	CLM_WW
				NEE				
Bias	-0.87	-0.37	-1.01	-0.61	-	-	-0.56	0.50
RMSE	6.34	4.96	7.73	7.58	-	-	3.80	3.27
r	-0.13	0.46	0.21	0.33	-	-	0.29	0.56
				LE				
Bias	-0.72	-0.13	-0.47	-0.23	-0.55	-0.09	-0.47	-0.77
RMSE	61.96	50.73	52.47	52.65	67.17	48.67	44.64	56.75
r	0.35	0.46	0.21	0.24	0.50	0.67	0.61	0.71
				H				
Bias	5.56	1.35	4.24	1.70	-8.49	-2.74	4.99	3.10
RMSE	45.97	27.63	40.93	39.94	47.26	32.81	49.30	35.08
r	0.42	0.50	0.45	0.48	0.21	0.36	0.47	0.63
				Rn				
Bias	-0.18	-0.05	-0.17	-0.13	-0.09	0.08	-0.03	-0.09
RMSE	36.11	38.01	47.28	45.15	37.34	46.43	45.17	44.49
r	0.80	0.81	0.68	0.69	0.78	0.97	0.71	0.73

4.2   Parameterization

490 In order to test the new parameter sets, CLM_WW was used. Since the modifications made in CLM_WW do not affect the considered CFTs (i.e. corn, sugar beet and potatoes), the findings discussed in this section result solely from the usage of modified parameterization.
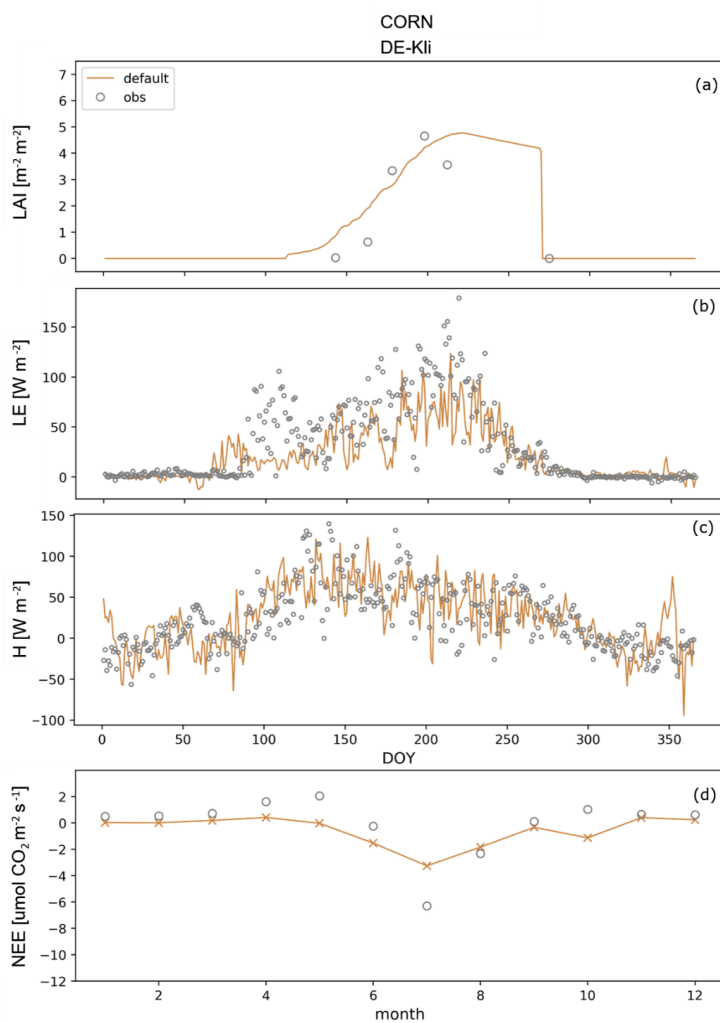
Figure 7: Daily simulation results of (a) LAI, (b) LE, (c) H, and (d) monthly NEE rates averaged over all corn years (see Table 6) at DE-Kli using the default parameterization (orange). Site observation data on LAI (all available observations plotted) and
495 fluxes (averaged over all respective years) are indicated in grey. Corresponding statistical analysis is listed in Table 6.

There is already a specific set of parameters available for the CFT temperate corn. This parameterization was tested for the site DE-Kli, where it resulted in a reasonable representation of seasonal LAI variation and magnitude (Figure 7). A moderate correlation was obtained for latent heat flux (0.56), with underestimation of latent heat flux

500 during the early growing cycle of corn, as well as for sensible heat flux (0.41). Similar to winter wheat at BE-Lon and DE-RuS, the simulated NEE shows a negative bias with an underestimation of peak NEE (Figure 7, Table 6). For the CFTs sugar beet and potatoes, the modified parameter set was tested for several years at BE-Lon and DE-RuS. The performance in reproducing seasonal variations and magnitudes of energy fluxes was strongly improved with the modified parameter set. Correspondingly, simulations with the modified parameter set for both sugar beet

505 and potatoes were able to reasonably capture seasonal variations and peak values of LAI as well as growth cycle length and harvest time (Figures 8 and 9). Whereas the default parameterization effectively reproduced the growth cycle and seasonal LAI variation of spring wheat, simulation results from the modified parameterizations better captured harvest date and growth cycle.

The improved growth cycle representation with modified parameters also led to more accurate simulation of

510 energy fluxes. For sugar beet at BE-Lon, the latent heat flux at peak LAI corresponds well with observed values while being underestimated before and after peak LAI and hence the sensible heat flux is overestimated at these times (Figure 8). Seasonal variations of energy fluxes and magnitudes were also captured much better in simulations with the modified parameterization. The simulations with modified parameters show slightly better net radiation correlations for both the sugar beet and potato CFTs at each site, compared to simulations with default

515 parameters (Table 6). The correlation between simulated and observed latent heat flux for sugar beet were strongly improved by changing the parameters (0.11 to 0.55 for DE-RuS and 0.21 to 0.55 for BE-Lon). The same is true for the simulated sensible heat flux for sugar beet (0.04 to 0.76 for DE-RuS and 0.08 to 0.51 for BE-Lon site). The NEE for the sugar beet CFT is underestimated during peak LAI periods for the default parameterization, resulting in poorer correlations compared to latent and sensible heat flux and net radiation (Figure 8). Simulations with the

520 modified parameter set resulted in a reduction in negative bias and reached higher correlation compared to the default parameterization (0.03 to 0.37 for DE-RuS and 0.05 to 0.64 for BE-Lon).

Similar improvements can be observed for the new potato parameterization while the correlation of simulation results with observation data is generally lower compared to the sugar beet CFT (Table 6). Seasonal LAI variations, growing cycle length and corresponding energy flux variations are improved in simulations with the modified

525 parameter set. Both the latent and the sensible heat flux are strongly improved at DE-RuS with correlation coefficients of 0.54 and 0.45 respectively for CLM_WW simulations. For BE-Lon, the improvement in correlation is slightly lower for both latent and sensible heat flux compared to DE-RuS. The seasonal variation of the NEE at BE-Lon is reasonably captured while monthly sums are overestimated with both parameterizations. The modified parameter set performed slightly better with an improved correlation of 0.58 compared to 0.43 with default

530 parameterization (Table 6).
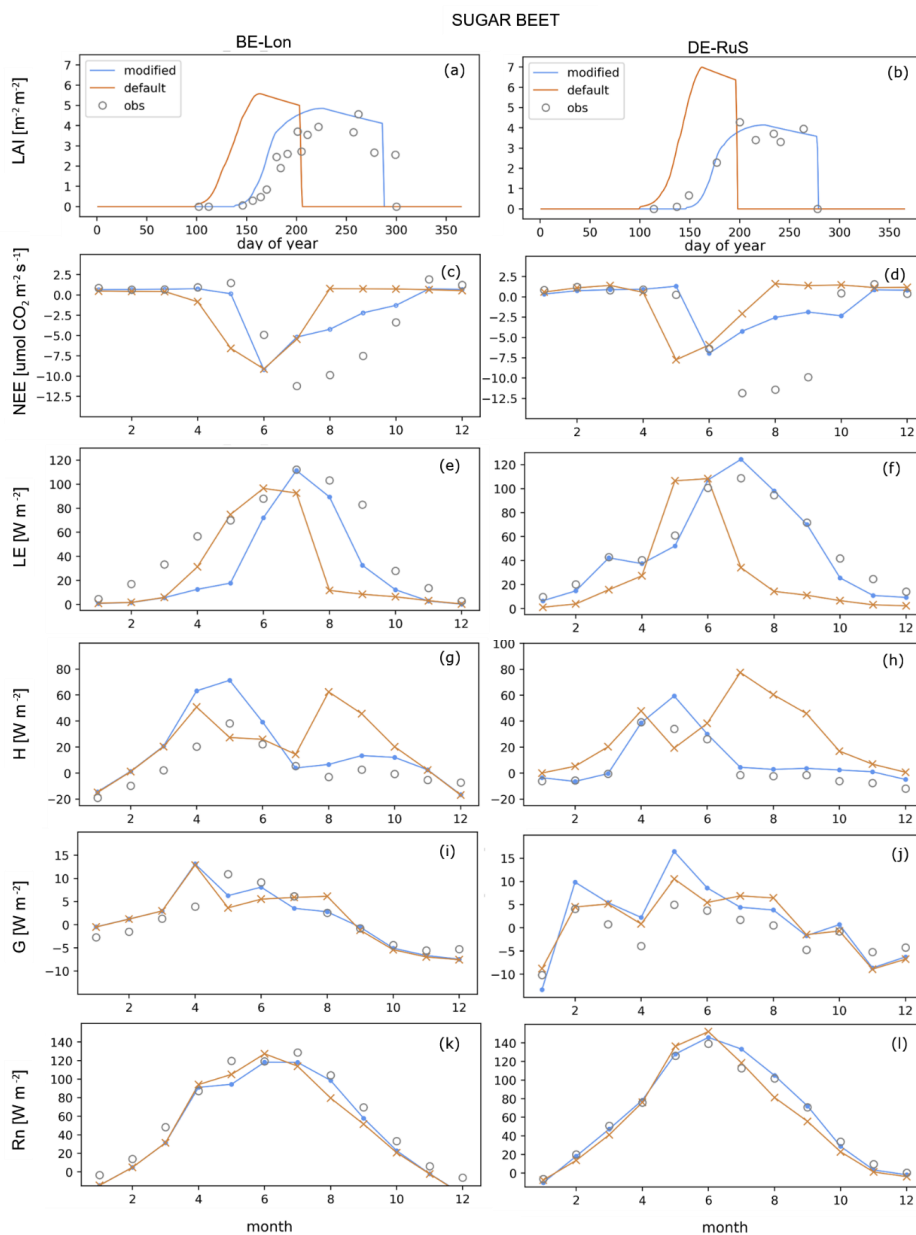
Figure 8: Simulation results of (a-b) LAI and monthly averaged simulation results of (c-d) NEE, (e-f) LE, (g-h) H, (i-j) G and (k-l) Rn for all sugar beet years (see Table 6) at the sites (left) BE-Lon and (right) DE-RuS. Simulation results for the default parameter set (orange) and the modified parameter set (blue) are compared to available site observations (grey) of LAI (all available observations plotted) and fluxes (averaged over all respective years). Corresponding performance statistics for daily simulation results are listed in Table 6.
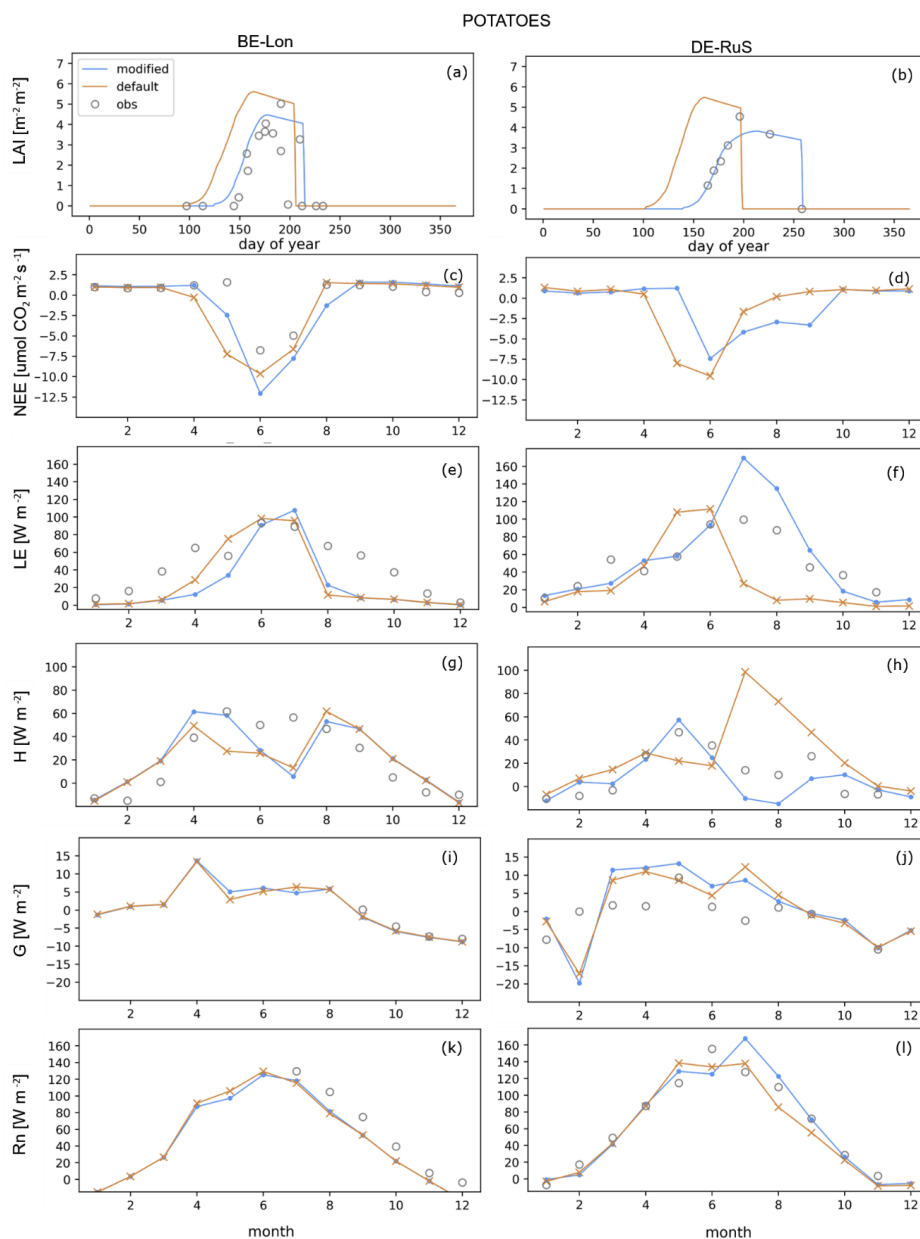
Figure 9: Simulation results of (a-b) LAI and monthly averaged simulation results of (c-d) NEE, (e-f) LE, (g-h) H, (i-j) G and
(k-l) Rn for all potatoes years (see Table 6) at the sites (left) BE-Lon and (right) DE-RuS. Simulation results run with the
default parameter set (orange) and the modified parameter set (blue) are compared to available site observations (grey) of LAI
(all available observations plotted) and fluxes (averaged over all respective years). Corresponding performance statistics for
daily simulation results are listed in Table 6.

Table 6: Bias, root mean square error (RMSE) and Pearson correlation coefficient (r) for the simulated daily NEE [µmol CO$_2$ W m^{-2} s^{-1}], LE [W m^{-2}], H [W m^{-2}] and Rn [W m^{-2}] using the default (*d*) and the modified parameterization (*m*) for the CFTs corn (only default), sugar beet and potatoes at the sites BE-Lon, DE-RuS, DE-RuM and DE-Kli respectively. Values were calculated for the time between recorded planting and harvest dates (averaged over all respective CFT years at each site) using simulation output and observation data at daily time step.

CFT	CORN	SUGARBEET				POTATOES			
Site	DE-Kli	DE-RuS		BE-Lon		DE-RuS		BE-Lon	
Year(s)	2007	2017		2008 2016		2019		2010 2014 2018	
Parameter set	*d*	*d*	*m*	*d*	*m*	*d*	*m*	*d*	*m*
NEE									
Bias	-1.00	-0.59	-0.75	0.05	-0.05	-	-	19.73	19.56
RMSE	2.59	9.10	5.94	6.19	3.75	-	-	5.24	5.21
r	0.46	-0.03	0.37	0.05	0.64	-	-	0.43	0.58
LE									
Bias	-0.33	-0.32	0.01	-0.37	-0.35	-0.28	0.25	0.26	0.09
RMSE	37.82	58.44	24.47	60.09	48.31	60.94	50.58	43.41	40.05
r	0.56	0.11	0.55	0.21	0.55	0.01	0.54	0.50	0.53
H									
Bias	-0.01	1.65	0.45	1.73	1.61	1.01	-0.38	0.50	0.22
RMSE	39.21	42.77	17.24	39.75	33.45	51.61	29.90	34.06	31.17
r	0.41	-0.04	0.76	-0.08	0.51	-0.10	0.45	0.18	0.31
Rn									
Bias	-0.12	-0.02	0.04	-0.11	-0.11	-0.04	0.04	-	-
RMSE	52.33	19.74	15.00	37.47	35.87	48.39	49.88	-	-
r	0.51	0.50	0.51	-0.22	-0.22	0.56	0.57	-	-

4.3 Cover cropping scheme

The cover cropping scheme was tested for two fields of application: (1) simulation of a second crop growth onset within one year and simulation of a cover crop, and (2) a more flexible crop rotation between different cash crops. To test the first application of CLM_WW_CC, we simulated the cash crop and cover crop rotation cycle at DE-RuS from 2016 to 2017 (Figure 11). A greening mix was planted in between the cash crop rotation of barley (adopted from the spring wheat CFT) in 2016 and sugar beet in 2017. While CLM_D simulated a perennial cycle of spring wheat, CLM_WW_CC was able to portray the crop rotation from barley to sugar beet in the following year as well as the coverage by a greening mix in between the cash crop cycles. Both, the simulation of a cover crop and the rotation of cash crops strongly improved the representation of LAI in CLM_WW_CC simulations over multiple years, especially during winter months (Figure 10). While in CLM_D simulations, the model assumed bare field conditions with no plant growth (LAI of 0) and very low latent heat flux, CLM_WW_CC simulated the plantation of a cover crop in fall of 2016, which leads to an increase in latent heat flux related to increased transpiration. Statistical evaluation of the simulated latent heat flux for the time window after harvest of the first cash crop from August 2016 to April 2017 shows that CLM_WW_CC reduced the negative bias from 0.74 to 0.13 compared to CLM_D simulation results, resulting in an RMSE reduction by approximately 42 % (Figure 10).
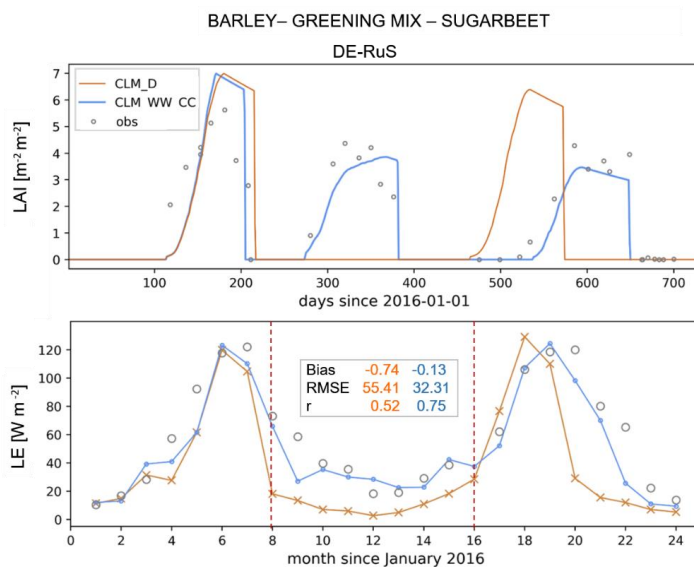
Figure 10: (Top) Simulated LAI for barley (2016), greening mix (2016/2017) and sugar beet (2017) rotation at DE-RuS and
570   (Bottom) corresponding monthly simulation results for the latent heat flux using the modified cover cropping subroutine
CLM_WW_CC (blue) compared to the default phenology algorithm of CLM_D (orange). Corresponding bias, RMSE and r
are given for the time window between the red dashed lines, calculated using simulation output and observation data at daily
time step. Available observation data is plotted in grey.

For the second case (DE-RuS), which represents a higher flexibility towards cash crop rotation, we simulated the
575   years of 2017 to 2019. Here, the crop rotation switched from sugar beet in 2017 to winter wheat in 2017/2018 to
potatoes in 2019 (Figure 11). While CLM_D was only capable of simulating a perennial spring wheat crop,
CLM_WW_CC was able to represent the rotation between different cash crops on the same field, which resulted
in a much better simulated LAI (by CLM_WW_CC) compared to CLM_D simulations. The improvement in
simulated energy fluxes is in accordance with the results presented in the previous chapters (4.1 and 4.2) where
580   results are analysed for each CFT respectively.
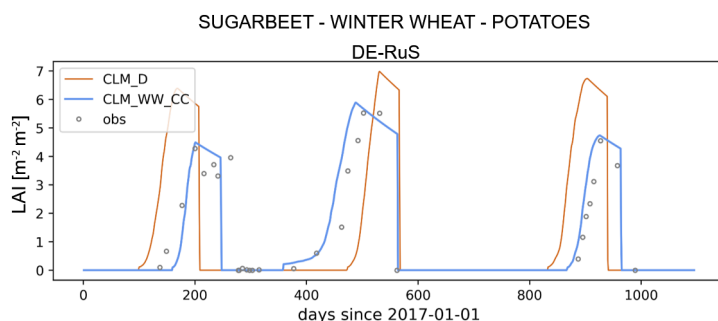
Figure 11: Simulated LAI for sugar beet (2017), winter wheat (2017/2018) and potatoes (2019) rotation at DE-RuS using the modified cover cropping subroutine CLM_WW_CC (blue) compared to simulation results for the same years with the default

585   phenology algorithm of CLM_D (orange). Available observation data is plotted in grey.

5   Discussion

All three modifications that were implemented in this study helped to improve the representation of cropland sites in CLM5. Similar to the findings of Lu et al. (2017) for CLM4.5, the implementation of their winter wheat routine resulted in a significant improvement in representing the seasonal LAI variations and surface energy fluxes during

590   winter wheat growth. Next to maize and rice, wheat is one of the most important international food crops and among the most important cash crops in Germany (22.8 million tons winter wheat yield in 2019 nation-wide (Statista, 2020)). In Germany and other western European countries, winter cereal varieties (e.g. winter rye, barley and wheat) are more abundant than summer cereals due to climatic conditions (Palosuo et al., 2011; Semenov and Shewry, 2011; Thaler et al., 2012).

595   Despite the general improvement of winter wheat growth and yield with the modified CLM_WW, there is still potential in further increasing the flexibility towards simulating different crop varieties and management practices. For example, the higher LAI captured at the DE-RuS site compared to BE-Lon was associated with a slightly higher simulated grain yield for DE-RuS, although recorded grain yield is lower compared to BE-LON (Table 4). This could be due to different management strategies such as fertilization application (timing, type and amount of

600   fertilizer) or the usage of different winter wheat varieties that can show different responses to e.g. water or heat stress, frost and have different grain productivities (White and Wilson, 2006; Bergkamp et al., 2018; Ceglar et al., 2019). Here, CLM5 is not flexible enough to represent the complex management practices concerning timing and type of fertilizer. In addition, CLM5 offers only one CFT for winter wheat representing all varieties. Whether this is an important limitation for regional or global scale simulations remains to be evaluated. In general, as already

605   noted by Lu et al. (2017), a more process based vernalization and cold tolerance routine would be useful to make this subroutine more applicable to other winter crops like rapeseed.

The observed overestimation of early LAI and underestimation of harvest date for winter wheat in CLM_WW (and CLM_D) simulations could be met by adjusting the minimum date for planting within the CFT parameterization. This could be useful to easily improve the crop cycle representation in regional simulations, where planting patterns are similar for larger agricultural areas. However it would restrict the flexibility of the

610   model to prognostically simulate planting dates.

In general, the simulated plant growth and resulting yield were highly sensitive to plant parameters that govern the growing degree calculation which in turn influence the phenological development and allocation of C and N. With only a limited number of CFTs in CLM, a discretization of plant parameters or varieties on a regional scale is not

615 possible at this point. A potential solution, without introducing additional CFT´s, could be to account for key parameters for each CFT varying with climate and soil conditions for large scale simulations (e.g. by gridded parameter sets). Furthermore, there is a need to evaluate and further discretise plant hydraulic properties (at this point one set of hydraulic parameters is applied to all types of crops) (Verhoef and Egea, 2014; Kennedy et al., 2017; Kennedy et al., 2019). This could play a major role in improving the quality of the yield prediction by the

620 model (Bassu et al., 2014; Daniel Kennedy et al., 2019). These plant hydraulic properties could be estimated by inverse modelling or data assimilation. In addition, data assimilation of e.g. in situ or remotely sensed soil moisture data and/or LAI could play a major role in increasing the accuracy of regional yield predictions (e.g. Guérif and Duke, 2000; Launay and Guerif, 2005; de Wit and van Diepen, 2007; Fang et al., 2008; Vazifedoust et al., 2009; Huang et al., 2015; Jin et al., 2018).

625 The default CLM5 does not account for the influence of weeds or cover crops and/or its litter on the carbon balance. There is a tool available for CLM5 that enables the simulation of transient land use and land cover changes (LULCC) (Lawrence et al., 2018). It was designed to simulate and study the effects of changing distributions of natural and crop vegetation, e.g. land use change from forest to agricultural fields (Lawrence et al., 2018), rather than inter-annual changes of agricultural management on crop vegetated areas. However, we found that it is not

630 applicable to regional scale simulations for all 78 available CFTs with customized changes in crop vegetation types. Furthermore, this tool changes the CFT of each column on the 1st of January every year according to prescribed values (customized). Thus, when using the CLM5 land-use change tool, for example to simulate the crop rotation from sugar beet in 2017 to winter wheat in 2017/2018 at DE-RuS, winter wheat would not be planted before fall 2017 (rather than in the same year as sugar beet is harvested) resulting in a long period of fallow field

635 when switching from summer to winter crop (Figure 12). Here, the implementation of our cover cropping routine enabled a second onset of plant growth within a year (including the switch to another CFT). This resulted in a pronounced improvement in LAI curves and latent heat flux, especially during winter months, by simulating the growth of a cover crop. It also proved to be beneficial in representing realistic agricultural field conditions by allowing crop rotations with higher flexibility than the default model. We anticipate that this modification will

640 allow a more realistic representation of seasonal LAI in ecosystems and agricultural regions where cover cropping and crop rotations are common management practices. The application of this routine is also of interest for areas with several cash crop cycles within a year like multiple annual crop cycles in India and China (Biradar and Xiao, 2011; Li et al., 2014; Sharma et al., 2015). We see further development potential for this routine and corresponding data sets to account for typical crop rotations and cover cropping scenarios for regional scale simulations (e.g. EU

645 regulations and goals on the adoption of cover crops for climate change mitigation (Smit et al., 2019)).

6   Conclusion

The default CLM5 was extended by adopting the winter wheat representation of Lu et al. (2017), by including crop specific parameterization for winter wheat, sugar beet and potatoes and by the addition of a cover cropping subroutine that allows several growth cycles within one year. The model modifications were tested for the

650 respective crops at four TERENO and ICOS cropland sites in Germany and Belgium, Selhausen (DE-RuS),

Merzenhausen (DE-RuM), Klingenberg (DE-Kli) and Lonzée (BE-Lon), for multiple years. The main results drawn from this study are as follows:

- The implementation of the winter wheat subroutines led to a significant simulation improvement in terms of energy fluxes, leaf area index, net ecosystem exchange and crop yield (reduction of underestimation from 80
655 – 90 % to 18 – 36 % at test site BE-Lon, good match for the test sites DE-RuS and DE-Kli in 2016 and slight overestimation at test site DE-Kli in 2011)

- The model performance was strongly improved with the modified crop parameter sets for sugar beet and potatoes: seasonal variations and magnitudes of energy fluxes and LAI were better reproduced with RMSE reduction during the crop cycle by up to 57 % for latent and 59 % for sensible heat flux at test site DE-RuS.

660 – In most cases the modification of CLM5 led to better reproduction of measured NEE at the test sites. However, the model showed a general weakness in reasonably simulating the NEE on agricultural fields, especially the peak value and post-harvest conditions.

- The implementation of our cover cropping routine enabled a second onset of plant growth within a year and thus was able to better capture realistic field conditions after harvest. Winter time RMSE for latent heat flux
665 was reduced by 42 %. Also, a higher flexibility in terms of crop rotations is now possible with CLM5.

We anticipate that our implementation of the winter wheat representation and specified parameterization will markedly improve yield predictions at regional scale for regions with a high abundance of winter cereal varieties. The cover cropping routine offers an improved basis on which to study the effects of large scale cover cropping on energy fluxes, soil water storage, soil carbon and nitrogen pools, as well as to investigate the role of different
670 cover crops as natural fertilizer in future studies with CLM5. A more realistic representation of post-harvest field conditions can play a crucial part in better representing the role of agriculture for regional and global energy and carbon fluxes and will be further developed and tested for regional scale simulations in future studies.

Despite our improvements, there is still a need to further develop certain functionalities and specific routines regarding the crop representation and land management in CLM5 in order to achieve better model performance
675 for agricultural land. Examples for improvements include: (1) a more detailed representation of agricultural management practices (e.g. tillage, C/N turnover, post-harvest surface conditions, fertilizer types and applications), (2) tools to account for spatial variability in plant physiological parameters, and (3) the discretization of plant hydraulic properties as opposed to using one parametrization for all crops.

7   Appendix

680 Table A1: Sowing and harvest dates at the ICOS and TERENO cropland study sites

Site code	Site	Years	Crop	Sowing	Harvest/plowing
DE-RuS	Selhausen	2015-2016	Winter barley	29.09.2015	10.07.2016
		2016	Catch crop	22.08.2016	06.01.2017
		2017	Sugar beet	31.03.2017	05.10.2017
		2017-2018	Winter wheat	25.10.2017	16.07.2018
		2019	Potato	26.04.2019	03.10.2019
DE-RuM	Merzenhausen	2016	Potato	12.04.2016	24.08.2016
		2016-2017	Winter wheat	17.10.2016	22.07.2017
		2017-2018	Rapeseed	30.08.2017	16.07.2018
DE-Kli	Klingenberg	2003-2004	Winter barley	06.09.2003	31.07.2004
		2004-2005	Rapeseed	18.08.2004	02.08.2005
		2005-2006	Winter wheat	25.09.2005	06.09.2006

		2007	Corn	23.04.2007	02.10.2007
		2008-2009	Winter barley	25.04.2008	27.08.2008
				12.09.2008	22.07.2009
		2009-2010	Rapeseed	25.08.2009	24.08.2010
		2010-2011	Winter wheat	02.10.2010	22.08.2011
		2012	Corn	25.04.2012	18.09.2012
		2013-2014	Winter barley	17.04.2013	24.08.2013
				01.10.2013	20.07.2014
		2014-2015	Rapeseed	21.08.2014	08.08.2015
		2015-2016	Winter wheat	18.09.2015	24.08.2016
		2016-2017	Radish and Brassica catch crop	01.09.2016	15.03.2017
		2017-2018	Winter barley	02.04.2017	25.08.2017
		2016-2017	Radish and Brassica catch crop	13.09.2017	13.04.2018
		2018	Corn	02.05.2018	04.09.2018
		2019	Bean	23.03.2019	18.08.2019
BE-Lon	Lonzée	2006-2007	Winter wheat	13.10.2006	05.08.2007
		2008	Sugar beet	22.04.2008	04.11.2008
		2008-2009	Winter wheat	13.11.2008	07.08.2009
		2009	Mustard	01.09.2009	01.12.2009
		2010	Potato	25.04.2010	05.09.2010
		2010-2011	Winter wheat	14.10.2010	16.08.2011
		2012	Corn	14.05.2012	13.10.2012
		2012-2013	Winter wheat	25.10.2012	12.08.2013
		2013	Mustard	05.09.2013	15.11.2013
		2014	Potato	07.04.2014	22.08.2014
		2014-2015	Winter wheat	15.10.2014	02.08.2015
		2015	Mustard	26.08.2015	09.12.2015
		2016	Sugar beet	12.04.2016	27.10.2016
		2016-2017	Winter wheat	29.10.2016	30.07.2017
		2017	Mustard	07.09.2017	08.12.2017
		2018	Potato	23.04.2018	11.09.2018
		2018-2019	Winter wheat	10.10.2018	01.08.2019

Table A2: Default (d) and modified (m) phenology and CN allocation parameters for the CFTs temperate corn, sugar beet and potatoes (both with default parameters for the CFT spring wheat) and winter wheat.

CFT		Temperate corn	Sugar beet		Potatoes		Winter wheat	
Parameter set		d	d	m	d	m	d	m
Variable	**Units**	*Phenology*						
min_NH_planting_date	MMDD	401	401	401	401	401	901	901
max_NH_planting_date	MMDD	615	615	530	615	530	1130	1130
planting_temp	K	283.15	280.15	280.15	280.15	277.15	1000	1000
min_planting_temp	K	279.15	272.15	272.15	272.15	272.15	283.15	283.15
gddmin	°days	50	50	60	50	60	50	100
mxmat	days	165	150	180	150	180	330	400
baset	°days	8	0	0	0	0	0	0
mxtmp	°C	30	26	30	26	30	26	26
hybgdd	-	1700	1700	2000	1700	2000	1700	2000
lfemerg	%	0.03	0.05	0.05	0.05	0.05	0.03	0.03
grnfill	%	0.65	0.6	0.65	0.6	0.65	0.4	0.6

Variable	Units							
ztopmx	m	2.5	1.2	0.5	1.2	0.5	1.2	1.2
laimx	m²/m²	5	7	6	7	6	7	7
slatop	m²/gC	0.05	0.035	0.02	0.035	0.02	0.035	0.028
Variable	**Units**	*CN ratios and allocation*						
leafcn	gC/gN	25	20	11	20	11	20	20
leafcn_min	gC/gN	15	15	8	15	8	15	15
leafcn_max	gC/gN	35	35	20	35	20	35	35
frootcn	gC/gN	42	42	42	42	42	42	43
graincn	gC/gN	50	50	50	50	50	50	15
flnr	fraction/gNm⁻²	0.29	0.41	0.15	0.41	0.15	0.41	0.3

685

Code availability. The modified model version CLM_WW_CC is available via GitHub: https://github.com/HPSCTerrSys/CTSM/tree/release-clm5.0-boas_ww_cc.

Data availability. For the TERENO sites Selhausen (TERENO ID: SE_EC_001 and SE_BK_001) and
690 Merzenhausen (TERENO ID: ME_EC_001, ME_BCK_001), all EC and meteorological data is freely available via the TERENO data portal TEODOOR (http://teodoor.icg.kfa-juelich.de/): Selhausen – ID SE_EC_001 doi:20.500.11952/TERENO/00000004; Selhausen – ID SE_BDK_001 doi:20.500.11952/TERENO/00000068; Merzenhausen – ID ME_EC_001 doi:20.500.11952/TERENO/00000434; Merzenhausen – ID ME_BCK_001 doi: 20.500.11952/TERENO/00000166. EC data for the ICOS study sites Lonzée (ICOS ID: BE-Lon) and Selhausen
695 (ICOS ID: DE-RuS) is available via the ICOS data portal (https://www.icos-cp.eu/). Additional data on vegetation and management practices (e.g. LAI, NDVI, canopy heights etc.) were kindly provided by the respective site operators.

Competing interests. The authors declare that they have no conflict of interest.

700

Author contribution. T. B. developed the modified model code, designed, performed and analysed the simulation experiments and prepared the manuscript with contributions from all co-authors. H.B., H.J.H.F., D.R., A.W. and H.V. supervised the research, co-designed the experiments and reviewed the manuscript. M. S., B. G. and B. H. performed pre-processing (e.g. quality control, gap-filling) of the respective site data.

705

Acknowledgements. The authors thankfully acknowledge Yaqiong Lu for providing the source code to the winter cereal implementation to CLM4.5 (Lu et al., 2017). Furthermore, the authors gratefully acknowledge the computing time granted on the supercomputer JURECA by the Jülich Supercomputing Centre (JSC). This study was partly funded by the Jülich-University of Melbourne Postgraduate Academy (JUMPA), an international
710 research collaboration between the University of Melbourne, Australia, and the Research Centre Jülich, Germany. This work used data acquired and shared by the TERENO project of the Helmholtz Association, the EU ICOS project of the European Research Infrastructure programme (ESFRI) and by the Deutsche Forschungsgemeinschaft (DFG, German Research Foundation) under Germany's Excellence Strategy - EXC 2070–390732324, project PhenoRob.

715

8   References

Aaheim, A., Amundsen, H., Dokken, T., and Wei, T. (2012). Impacts and adaptation to climate change in European economies. Global Environmental Change, 22(4), 959–968. https://doi.org/10.1016/j.gloenvcha.2012.06.005

720   Barlow, K. M., Christy, B. P., O'Leary, G. J., Riffkin, P. A., and Nuttall, J. G. (2015). Simulating the impact of extreme heat and frost events on wheat crop production: A review. Field Crops Research, 171, 109–119. https://doi.org/10.1016/j.fcr.2014.11.010

Basche, Archontoulis, S. V., Kaspar, T. C., Jaynes, D. B., Parkin, T. B., and Miguez, F. E. (2016). Simulating long-term impacts of cover crops and climate change on crop production and environmental outcomes in
725   the Midwestern United States. Agriculture, Ecosystems and Environment, 218, 95–106. https://doi.org/10.1016/j.agee.2015.11.011

Basche, Miguez, F. E., Kaspar, T. C., and Castellano, M. J. (2014). Do cover crops increase or decrease nitrous oxide emissions? A meta-analysis. Journal of Soil and Water Conservation, 69(6), 471–482. https://doi.org/10.2489/jswc.69.6.471

730   Bassu, S., Brisson, N., Durand, J. L., Boote, K., Lizaso, J., Jones, J. W., Rosenzweig, C., Ruane, A. C., Adam, M., Baron, C., Basso, B., Biernath, C., Boogaard, H., Conijn, S., Corbeels, M., Deryng, D., Sanctis, G. D., Gayler, S., Grassini, P., … Waha, K. (2014). How do various maize crop models vary in their responses to climate change factors? Global Change Biology, 20(7), 2301–2320. https://doi.org/10.1111/gcb.12520

Bergjord, A. K., Bonesmo, H., and Skjelvåg, A. O. (2008). Modelling the course of frost tolerance in winter wheat:
735   I. Model development. European Journal of Agronomy, 28(3), 321–330. https://doi.org/10.1016/j.eja.2007.10.002

Bergkamp, B., Impa, S. M., Asebedo, A. R., Fritz, A. K., and Jagadish, S. V. K. (2018). Prominent winter wheat varieties response to post-flowering heat stress under controlled chambers and field based heat tents. Field Crops Research, 222, 143–152. https://doi.org/10.1016/j.fcr.2018.03.009

740   Biradar, C. M., and Xiao, X. (2011). Quantifying the area and spatial distribution of double- and triple-cropping croplands in India with multi-temporal MODIS imagery in 2005. International Journal of Remote Sensing, 32(2), 367–386. https://doi.org/10.1080/01431160903464179

Bogena, H. R., Montzka, C., Huisman, J. A., Graf, A., Schmidt, M., Stockinger, M., von Hebel, C., Hendricks-Franssen, H. J., van der Kruk, J., Tappe, W., Lücke, A., Baatz, R., Bol, R., Groh, J., Pütz, T., Jakobi, J.,
745   Kunkel, R., Sorg, J., and Vereecken, H. (2018). The TERENO-Rur Hydrological Observatory: A Multiscale Multi-Compartment Research Platform for the Advancement of Hydrological Science. Vadose Zone Journal, 17(1). https://doi.org/10.2136/vzj2018.03.0055

Buysse, P., Manise, Bodson, Alain, Debacq, De, A., Ligne, Bernard, Heinesch, Tanguy, Manise, Christine, Moureaux, Marc, and Aubinet. (2017). Carbon budget measurement over 12 years at a crop production
750   site in the silty-loam region in Belgium. Agricultural and Forest Meteorology. http://agris.fao.org/agris-search/search.do?recordID=US201700215651

Carrer, D., Pique, G., Ferlicoq, M., Ceamanos, X., and Ceschia, E. (2018). What is the potential of cropland albedo management in the fight against global warming? A case study based on the use of cover crops. Environmental Research Letters, 13(4), 044030. https://doi.org/10.1088/1748-9326/aab650

755   Ceglar, A., van der Wijngaart, R., de Wit, A., Lecerf, R., Boogaard, H., Seguini, L., van den Berg, M., Toreti, A., Zampieri, M., Fumagalli, D., and Baruth, B. (2019). Improving WOFOST model to simulate winter wheat

phenology in Europe: Evaluation and effects on yield. Agricultural Systems, 168, 168–180. https://doi.org/10.1016/j.agsy.2018.05.002

Challinor, A. J., Watson, J., Lobell, D. B., Howden, S. M., Smith, D. R., and Chhetri, N. (2014). A meta-analysis of crop yield under climate change and adaptation. Nature Climate Change, 4(4), 287–291. https://doi.org/10.1038/nclimate2153

Cheng, Y., Huang, M., Chen, M., Guan, K., Bernacchi, C., Peng, B., and Tan, Z. (2020). Parameterizing Perennial Bioenergy Crops in Version 5 of the Community Land Model Based on Site-Level Observations in the Central Midwestern United States. Journal of Advances in Modeling Earth Systems, 12(1), e2019MS001719. https://doi.org/10.1029/2019MS001719

Chouard, P. (1960). Vernalization and its Relations to Dormancy. Annual Review of Plant Physiology, 11(1), 191–238. https://doi.org/10.1146/annurev.pp.11.060160.001203

de Wit, A. J. W., and van Diepen, C. A. (2007). Crop model data assimilation with the Ensemble Kalman filter for improving regional crop yield forecasts. Agricultural and Forest Meteorology, 146(1), 38–56. https://doi.org/10.1016/j.agrformet.2007.05.004

Deryng, D., Conway, D., Ramankutty, N., Price, J., and Warren, R. (2014). Global crop yield response to extreme heat stress under multiple climate change futures. Environmental Research Letters, 9(3), 034011. https://doi.org/10.1088/1748-9326/9/3/034011

Eder, F., Schmidt, M., Damian, T., Träumner, K., and Mauder, M. (2015). Mesoscale Eddies Affect Near-Surface Turbulent Exchange: Evidence from Lidar and Tower Measurements. Journal of Applied Meteorology and Climatology, 54(1), 189–206. https://doi.org/10.1175/JAMC-D-14-0140.1

Fang, H., Liang, S., Hoogenboom, G., Teasdale, J., and Cavigelli, M. (2008). Corn-yield estimation through assimilation of remotely sensed data into the CSM-CERES-Maize model. International Journal of Remote Sensing, 29(10), 3011–3032. https://doi.org/10.1080/01431160701408386

Fisher, R. A., Wieder, W. R., Sanderson, B. M., Koven, C. D., Oleson, K. W., Xu, C., Fisher, J. B., Shi, M., Walker, A. P., and Lawrence, D. M. (2019). Parametric Controls on Vegetation Responses to Biogeochemical Forcing in the CLM5. Journal of Advances in Modeling Earth Systems, 11(9), 2879–2895. https://doi.org/10.1029/2019MS001609

Gosling, S. N. (2013). The likelihood and potential impact of future change in the large-scale climate-earth system on ecosystem services. Environmental Science and Policy, 27, S15–S31. https://doi.org/10.1016/j.envsci.2012.03.011

Graf, A., Klosterhalfen, A., Arriga, N., Bernhofer, C., Bogena, H. R., Bornet, F., Brüggemann, N., Brümmer, C., Chi, J., Cremonese, E., Cuntz, M., Dusek, J., El-Madany, T., Fares, S., Fischer, M., Foltynova, L., Gielen, B., Gottschalt, P., Gharun, M., … Vereecken, H. (in review). Altered energy partitioning across terrestrial ecosystems in the European drought year 2018.

Graf, Alexander. (2017). Gap-filling meteorological variables with Empirical Orthogonal Functions. 19, 8491.

Guérif, M., and Duke, C. L. (2000). Adjustment procedures of a crop model to the site specific characteristics of soil and crop using remote sensing data assimilation. Agriculture, Ecosystems and Environment, 81(1), 57–69. https://doi.org/10.1016/S0167-8809(00)00168-7

Han, X., Franssen, H.-J. H., Montzka, C., and Vereecken, H. (2014). Soil moisture and soil properties estimation in the Community Land Model with synthetic brightness temperature observations. Water Resources

Research, 6081–6105. https://doi.org/10.1002/2013WR014586@10.1002/(ISSN)1944-7973.SVASYST1

Huang, J., Tian, L., Liang, S., Ma, H., Becker-Reshef, I., Huang, Y., Su, W., Zhang, X., Zhu, D., and Wu, W.
800   (2015). Improving winter wheat yield estimation by assimilation of the leaf area index from Landsat TM
       and MODIS data into the WOFOST model. Agricultural and Forest Meteorology, 204, 106–121.
       https://doi.org/10.1016/j.agrformet.2015.02.001

Hunter, M. C., White, C. M., Kaye, J. P., and Kemanian, A. R. (2019). Ground-Truthing a Recent Report of Cover
       Crop–Induced Winter Warming. Agricultural and Environmental Letters, 4(1).
805   https://doi.org/10.2134/ael2019.03.0007

ICOS. (2020). Integrated Carbon Observation System Carbon Portal. https://www.icos-cp.eu/

Jin, X., Kumar, L., Li, Z., Feng, H., Xu, X., Yang, G., and Wang, J. (2018). A review of data assimilation of remote
       sensing and crop models. European Journal of Agronomy, 92, 141–152.
       https://doi.org/10.1016/j.eja.2017.11.002

810   Kaye, J. P., and Quemada, M. (2017). Using cover crops to mitigate and adapt to climate change. A review.
       Agronomy for Sustainable Development, 37(1), 4. https://doi.org/10.1007/s13593-016-0410-x

Kennedy, D., Swenson, S. C., Oleson, K. W., Lawrence, D. M., Fisher, R., and Gentine, P. (2017). Representing
       Plant Hydraulics in a Global Model: Updates to the Community Land Model. AGU Fall Meeting
       Abstracts, 12. http://adsabs.harvard.edu/abs/2017AGUFM.B12D..05K

815   Kennedy, Daniel, Swenson, S., Oleson, K. W., Lawrence, D. M., Fisher, R., Costa, A. C. L. da, and Gentine, P.
       (2019). Implementing Plant Hydraulics in the Community Land Model, Version 5. Journal of Advances
       in Modeling Earth Systems, 11(2), 485–513. https://doi.org/10.1029/2018MS001500

Kucharik, C. J. (2008). Contribution of Planting Date Trends to Increased Maize Yields in the Central United
       States. Agronomy Journal, 100(2), 328–336. https://doi.org/10.2134/agronj2007.0145

820   Kucharik, C. J., Barford, C. C., Maayar, M. E., Wofsy, S. C., Monson, R. K., and Baldocchi, D. D. (2006). A
       multiyear evaluation of a Dynamic Global Vegetation Model at three AmeriFlux forest sites: Vegetation
       structure, phenology, soil temperature, and CO2 and H2O vapor exchange. Ecological Modelling, 196(1),
       1–31. https://doi.org/10.1016/j.ecolmodel.2005.11.031

Kucharik, C. J., and Brye, K. R. (2003). Integrated BIosphere Simulator (IBIS) Yield and Nitrate Loss Predictions
825   for Wisconsin Maize Receiving Varied Amounts of Nitrogen Fertilizer. Journal of Environmental
       Quality, 32(1), 247–268. https://doi.org/10.2134/jeq2003.2470

Kutsch, W. L., Aubinet, M., Buchmann, N., Smith, P., Osborne, B., Eugster, W., Wattenbach, M., Schrumpf, M.,
       Schulze, E. D., Tomelleri, E., Ceschia, E., Bernhofer, C., Béziat, P., Carrara, A., Di Tommasi, P.,
       Grünwald, T., Jones, M., Magliulo, V., Marloie, O., … Ziegler, W. (2010). The net biome production of
830   full crop rotations in Europe. Agriculture, Ecosystems and Environment, 139(3), 336–345.
       https://doi.org/10.1016/j.agee.2010.07.016

Launay, M., and Guerif, M. (2005). Assimilating remote sensing data into a crop model to improve predictive
       performance for spatial applications. Agriculture, Ecosystems and Environment, 111(1–4), 321–339.
       https://doi.org/10.1016/j.agee.2005.06.005

835   Lawrence, David M., Oleson, K. W., Flanner, M. G., Thornton, P. E., Swenson, S. C., Lawrence, P. J., Zeng, X.,
       Yang, Z.-L., Levis, S., Sakaguchi, K., Bonan, G. B., and Slater, A. G. (2011). Parameterization

improvements and functional and structural advances in Version 4 of the Community Land Model. Journal of Advances in Modeling Earth Systems, 3(1). https://doi.org/10.1029/2011MS00045

840   Lawrence, D.M., Fisher, R., Koven, C., Oleson, K., Svenson, S., Vertenstein, M., and et al. (2018). Technical Description of version 5.0 of the Community Land Model (CLM). The National Center for Atmospheric Research (NCAR). http://www.cesm.ucar.edu/models/cesm2/land/CLM50_Tech_Note.pdf

Lawrence, P., Lawrence, D. M., Hurtt, G. C., and Calvin, K. V. (2019). Advancing our understanding of the impacts of historic and projected land use in the Earth System: The Land Use Model Intercomparison Project (LUMIP). AGU Fall Meeting Abstracts, 23.
845   http://adsabs.harvard.edu/abs/2019AGUFMGC23B..01L

Leng, G., Huang, M., Tang, Q., Sacks, W. J., Lei, H., and Leung, L. R. (2013). Modeling the effects of irrigation on land surface fluxes and states over the conterminous United States: Sensitivity to input data and model parameters. Journal of Geophysical Research: Atmospheres, 118(17), 9789–9803. https://doi.org/10.1002/jgrd.50792

850   Levis, S., Badger, A., Drewniak, B., Nevison, C., and Ren, X. (2018). CLMcrop yields and water requirements: Avoided impacts by choosing RCP 4.5 over 8.5. Climatic Change, 146(3), 501–515. https://doi.org/10.1007/s10584-016-1654-9

Levis, S., Bonan, G. B., Kluzek, E., Thornton, P. E., Jones, A., Sacks, W. J., and Kucharik, C. J. (2012). Interactive Crop Management in the Community Earth System Model (CESM1): Seasonal Influences on Land–
855   Atmosphere Fluxes. Journal of Climate, 25(14), 4839–4859. https://doi.org/10.1175/JCLI-D-11-00446.1

Li, L., Friedl, M. A., Xin, Q., Gray, J., Pan, Y., and Frolking, S. (2014). Mapping Crop Cycles in China Using MODIS-EVI Time Series. Remote Sensing, 6(3), 2473–2493. https://doi.org/10.3390/rs6032473

Lobell, Bala, G., and Duffy, P. B. (2006). Biogeophysical impacts of cropland management changes on climate. Geophysical Research Letters, 33(6). https://doi.org/10.1029/2005GL025492

860   Lobell, Schlenker, W., and Costa-Roberts, J. (2011). Climate Trends and Global Crop Production Since 1980. Science, 333(6042), 616–620. https://doi.org/10.1126/science.1204531

Lombardozzi, D. L., Bonan, G. B., Wieder, W., Grandy, A. S., Morris, C., and Lawrence, D. L. (2018). Cover Crops May Cause Winter Warming in Snow-Covered Regions. Geophysical Research Letters, 45(18), 9889–9897. https://doi.org/10.1029/2018GL079000

865   Lu, Y., Williams, I. N., Bagley, J. E., Torn, M. S., and Kueppers, L. M. (2017). Representing winter wheat in the Community Land Model (version 4.5). Geoscientific Model Development, 10(5), 1873–1888. https://doi.org/10.5194/gmd-10-1873-2017

Ma, S., Churkina, G., and Trusilova, K. (2012). Investigating the impact of climate change on crop phenological events in Europe with a phenology model. International Journal of Biometeorology, 56(4), 749–763.
870   https://doi.org/10.1007/s00484-011-0478-6

Möller, K., and Reents, H.-J. (2009). Effects of various cover crops after peas on nitrate leaching and nitrogen supply to succeeding winter wheat or potato crops. Journal of Plant Nutrition and Soil Science, 172(2), 277–287. https://doi.org/10.1002/jpln.200700336

Moureaux, C. (2006). Annual net ecosystem carbon exchange by a sugar beet crop. Agricultural and Forest
875   Meteorology, 139(1), 25–39. https://doi.org/10.1016/j.agrformet.2006.05.009

Moureaux, C., Debacq, A., Hoyaux, J., Suleau, M., Tourneur, D., Vancutsem, F., Bodson, B., and Aubinet, M. (2008). Carbon balance assessment of a Belgian winter wheat crop (Triticum aestivum L.). Global Change Biology, 14(6), 1353–1366. https://doi.org/10.1111/j.1365-2486.2008.01560.x

Naz, B. S., Kurtz, W., Montzka, C., Sharples, W., Goergen, K., Keune, J., Gao, H., Springer, A., Hendricks Franssen, H.-J., and Kollet, S. (2019). Improving soil moisture and runoff simulations at 3 km over Europe using land surface data assimilation. Hydrology and Earth System Sciences, 23(1), 277–301. https://doi.org/10.5194/hess-23-277-2019

Ney, P., and Graf, A. (2018). High-Resolution Vertical Profile Measurements for Carbon Dioxide and Water Vapour Concentrations Within and Above Crop Canopies. Boundary-Layer Meteorology, 166(3), 449–473. https://doi.org/10.1007/s10546-017-0316-4

Niu, G.-Y., Yang, Z.-L., Mitchell, K. E., Chen, F., Ek, M. B., Barlage, M., Kumar, A., Manning, K., Niyogi, D., Rosero, E., Tewari, M., and Xia, Y. (2011). The community Noah land surface model with multiparameterization options (Noah-MP): 1. Model description and evaluation with local-scale measurements. Journal of Geophysical Research: Atmospheres, 116(D12). https://doi.org/10.1029/2010JD015139

Olesen, J. E., Trnka, M., Kersebaum, K. C., Skjelvåg, A. O., Seguin, B., Peltonen-Sainio, P., Rossi, F., Kozyra, J., and Micale, F. (2011). Impacts and adaptation of European crop production systems to climate change. European Journal of Agronomy, 34(2), 96–112. https://doi.org/10.1016/j.eja.2010.11.003

Oleson, K. W., Lawrence, D. M., B, G., Flanner, M. G., Kluzek, E., J, P., Levis, S., Swenson, S. C., Thornton, E., Feddema, J., Heald, C. L., Lamarque, J., Niu, G., Qian, T., Running, S., Sakaguchi, K., Yang, L., Zeng, X., Zeng, X., and Decker, M. (2010). Technical Description of version 4.0 of the Community Land Model (CLM).

Ozdogan, M., Rodell, M., Beaudoing, H. K., and Toll, D. L. (2010). Simulating the Effects of Irrigation over the United States in a Land Surface Model Based on Satellite-Derived Agricultural Data. Journal of Hydrometeorology, 11(1), 171–184. https://doi.org/10.1175/2009JHM1116.1

Palosuo, T., Kersebaum, K. C., Angulo, C., Hlavinka, P., Moriondo, M., Olesen, J. E., Patil, R. H., Ruget, F., Rumbaur, C., Takáč, J., Trnka, M., Bindi, M., Çaldağ, B., Ewert, F., Ferrise, R., Mirschel, W., Şaylan, L., Šiška, B., and Rötter, R. (2011). Simulation of winter wheat yield and its variability in different climates of Europe: A comparison of eight crop growth models. European Journal of Agronomy, 35(3), 103–114. https://doi.org/10.1016/j.eja.2011.05.001

Peel, M. C., Finlayson, B. L., and Mcmahin, T. A. (2007). Updated world map of the Köppen-Geiger climate classification. Hydrology and Earth System Sciences Discussions, European Geosciences Union, 4(2), 439–473.

Plaza-Bonilla, D., Nolot, J.-M., Raffaillac, D., and Justes, E. (2015). Cover crops mitigate nitrate leaching in cropping systems including grain legumes: Field evidence and model simulations. Agriculture, Ecosystems and Environment, 212, 1–12. https://doi.org/10.1016/j.agee.2015.06.014

Post, H., Vrugt, J. A., Fox, A., Vereecken, H., and Hendricks-Franssen, H.-J. (2017). Estimation of Community Land Model parameters for an improved assessment of net carbon fluxes at European sites. Journal of Geophysical Research: Biogeosciences, 122(3), 661–689. https://doi.org/10.1002/2015JG003297

915 Prescher, A.-K., Grünwald, T., and Bernhofer, C. (2010). Land use regulates carbon budgets in eastern Germany: From NEE to NBP. Agricultural and forest meteorology, 150(7–8), 1016–1025. https://doi.org/10.1016/j.agrformet.2010.03.008

Reichenau, T. G., Korres, W., Schmidt, M., Graf, A., Welp, G., Meyer, N., Stadler, A., Brogi, C., and Schneider, K. (2020). A comprehensive dataset of vegetation states, fluxes of matter and energy, weather,
920 agricultural management, and soil properties from intensively monitored crop sites in Western Germany. Earth System Science Data Discussions, 1–59. https://doi.org/10.5194/essd-2019-193

Rosenzweig, C., Elliott, J., Deryng, D., Ruane, A. C., Müller, C., Arneth, A., Boote, K. J., Folberth, C., Glotter, M., Khabarov, N., Neumann, K., Piontek, F., Pugh, T. A. M., Schmid, E., Stehfest, E., Yang, H., and Jones, J. W. (2014). Assessing agricultural risks of climate change in the 21st century in a global gridded
925 crop model intercomparison. Proceedings of the National Academy of Sciences, 111(9), 3268–3273. https://doi.org/10.1073/pnas.1222463110

Sainju, U. M., Whitehead, W. F., and Singh, B. P. (2003). Cover crops and nitrogen fertilization effects on soil aggregation and carbon and nitrogen pools. Canadian Journal of Soil Science, 83(2), 155–165. https://doi.org/10.4141/S02-056

930 Sánchez-Sastre, L. F., Martín-Ramos, P., Navas-Gracia, L. M., Hernández-Navarro, S., and Martín-Gil, J. (2018). Impact of Climatic Variables on Carbon Content in Sugar Beet Root. Agronomy, 8(8), 147. https://doi.org/10.3390/agronomy8080147

Semenov, M. A., and Shewry, P. R. (2011). Modelling predicts that heat stress, not drought, will increase vulnerability of wheat in Europe. Scientific Reports, 1(1), 1–5. https://doi.org/10.1038/srep00066

935 Sharma, S. D., Kumar, P., Bhardwaj, S. K., and Chandel, A. (2015). Agronomic performance, nutrient cycling and microbial biomass in soil as affected by pomegranate based multiple crop sequencing. Scientia Horticulturae, 197, 504–515. https://doi.org/10.1016/j.scienta.2015.10.013

Sheng, M., Liu, J., Zhu, A.-X., Rossiter, D. G., Zhu, L., and Peng, G. (2018). Evaluation of CLM-Crop for maize growth simulation over Northeast China. Ecological Modelling, 377, 26–34.
940 https://doi.org/10.1016/j.ecolmodel.2018.03.005

Smit, B., Janssens, B., Haagsma, W., Hennen, W., Adrados Jose, L., and Kathage, J. (2019). Adoption of cover crops for climate change mitigation in the EU (JRC116730) [EUR - Scientific and Technical Research Reports]. Publications Office of the European Union. https://publications.jrc.ec.europa.eu/repository/handle/111111111/57996

945 Statista. (2020). Yield statistics of winter wheat for Germany from 2006 to 2019. https://de.statista.com/statistik/daten/studie/262303/umfrage/erntemenge-von-weizen-in-deutschland/

Stehfest, E., Heistermann, M., Priess, J. A., Ojima, D. S., and Alcamo, J. (2007). Simulation of global crop production with the ecosystem model DayCent. Ecological Modelling, 209(2), 203–219. https://doi.org/10.1016/j.ecolmodel.2007.06.028

950 Streck, N. A., Weiss, A., and Baenziger, P. S. (2003). A Generalized Vernalization Response Function for Winter Wheat. Agronomy Journal, 95(1), 155–159. https://doi.org/10.2134/agronj2003.1550

Sulis, M., Langensiepen, M., Shrestha, P., Schickling, A., Simmer, C., and Kollet, S. J. (2015). Evaluating the Influence of Plant-Specific Physiological Parameterizations on the Partitioning of Land Surface Energy Fluxes. Journal of Hydrometeorology, 16(2), 517–533. https://doi.org/10.1175/JHM-D-14-0153.1

955   Tai, A. P. K., Martin, M. V., and Heald, C. L. (2014). Threat to future global food security from climate change
        and ozone air pollution. Nature Climate Change, 4(9), 817–821. https://doi.org/10.1038/nclimate2317

        Thaler, S., Eitzinger, J., Trnka, M., and Dubrovsky, M. (2012). Impacts of climate change and alternative
        adaptation options on winter wheat yield and water productivity in a dry climate in Central Europe. The
        Journal of Agricultural Science, 150(5), 537–555. https://doi.org/10.1017/S0021859612000093

960   Thornton, P. E., and Rosenbloom, N. A. (2005). Ecosystem model spin-up: Estimating steady state conditions in
        a coupled terrestrial carbon and nitrogen cycle model. Ecological Modelling, 189(1), 25–48.
        https://doi.org/10.1016/j.ecolmodel.2005.04.008

        Tiemann, L. K., Grandy, A. S., Atkinson, E. E., Marin-Spiotta, E., and McDaniel, M. D. (2015). Crop rotational
        diversity enhances belowground communities and functions in an agroecosystem. Ecology Letters, 18(8),
965   761–771. https://doi.org/10.1111/ele.12453

        Twine, T. E., and Kucharik, C. J. (2009). Climate impacts on net primary productivity trends in natural and
        managed ecosystems of the central and eastern United States. Agricultural and Forest Meteorology,
        149(12), 2143–2161. https://doi.org/10.1016/j.agrformet.2009.05.012

        Urban, D., Roberts, M. J., Schlenker, W., and Lobell, D. B. (2012). Projected temperature changes indicate
970   significant increase in interannual variability of U.S. maize yields. Climatic Change, 112(2), 525–533.
        https://doi.org/10.1007/s10584-012-0428-2

        Van den Hoof, C., Hanert, E., and Vidale, P. L. (2011). Simulating dynamic crop growth with an adapted land
        surface model – JULES-SUCROS: Model development and validation. Agricultural and Forest
        Meteorology, 151(2), 137–153. https://doi.org/10.1016/j.agrformet.2010.09.011

975   Vazifedoust, M., Dam, J. C. van, Bastiaanssen, W. G. M., and Feddes, R. A. (2009). Assimilation of satellite data
        into agrohydrological models to improve crop yield forecasts. International Journal of Remote Sensing,
        30(10), 2523–2545. https://doi.org/10.1080/01431160802552769

        Verhoef, A., and Egea, G. (2014). Modeling plant transpiration under limited soil water: Comparison of different
        plant and soil hydraulic parameterizations and preliminary implications for their use in land surface
980   models.   Agricultural   and   Forest   Meteorology,   191,   22–32.
        https://doi.org/10.1016/j.agrformet.2014.02.009

        Vico, G., Hurry, V., and Weih, M. (2014). Snowed in for survival: Quantifying the risk of winter damage to
        overwintering field crops in northern temperate latitudes. Agricultural and Forest Meteorology, 197, 65–
        75. https://doi.org/10.1016/j.agrformet.2014.06.003

985   Webler, G., Roberti, D. R., Cuadra, S. V., Moreira, V. S., and Costa, M. H. (2012). Evaluation of a Dynamic
        Agroecosystem Model (Agro-IBIS) for Soybean in Southern Brazil. Earth Interactions, 16(12), 1–15.
        https://doi.org/10.1175/2012EI000452.1

        White, E. M., and Wilson, F. E. A. (2006). Responses of Grain Yield, Biomass and Harvest Index and Their Rates
        of Genetic Progress to Nitrogen Availability in Ten Winter Wheat Varieties. Irish Journal of Agricultural
990   and Food Research, 45(1), 85–101. JSTOR.

        Whitmore, A. P., and Groot, J. J. R. (1997). The decomposition of sugar beet residues: Mineralization versus
        immobilization   in   contrasting   soil   types.   Plant   and   Soil,   192(2),   237–247.
        https://doi.org/10.1023/A:1004288828793

Wutzler, T., Lucas-Moffat, A., Migliavacca, M., Knauer, J., Sickel, K., Šigut, L., Menzer, O., and Reichstein, M.

995   (2018). Basic and extensible post-processing of eddy covariance flux data with REddyProc. Biogeosciences, 15(16), 5015–5030. https://doi.org/10.5194/bg-15-5015-2018

Xu, H., Twine, T. E., and Girvetz, E. (2016). Climate Change and Maize Yield in Iowa. PLOS ONE, 11(5), e0156083. https://doi.org/10.1371/journal.pone.0156083

Zheng, H., Wang, Y., Zhao, J., Shi, X., Ma, Z., and Fan, M. (2018). Tuber formation as influenced by the C: N

1000   ratio in potato plants. Journal of Plant Nutrition and Soil Science, 181(5), 686–693. https://doi.org/10.1002/jpln.201700571